ESTIMATION OF FLUID FUGACITIES IN OROGENIC MANTLE PERIDOTITES

A Thesis

by

THOMAS FREDERICK CUMMINGS

Submitted to the Office of Graduate and Professional Studies of
Texas A&M University
in partial fulfillment of the requirements for the degree of

MASTER OF SCIENCE

Chair of Committee,	William Lamb
Committee Members,	Franco Marcantonio
	Julie Newman
Head of Department,	Julie Newman

December 2019

Major Subject: Geology

ABSTRACT

Water (H_2O and H-species in minerals) has a strong influence on many physio-chemical properties of upper mantle rocks (e.g. viscosity, melting temperature, thermal conductivity). Estimates of mantle water contents are often based on measuring the concentration of H in nominally anhydrous minerals (NAMs) contained in peridotites. However, these NAMs may suffer diffusive loss of H during emplacement at the Earth's surface, and the relationship between NAM H contents and H_2O fugacities are not well known for all mantle NAMs. In this study, fluid-buffering mineral equilibria are used to estimate the fugacities of various fluid species in peridotites.

The compositions of co-existing minerals from nine orogenic peridotites were determined via electron microprobe. These samples were from six different locations (New Caledonia; Bestiac, Lherz, and Turon de Técouère, France; Almklovdalen, Norway; and the Trinity Ophiolite, CA USA), and contain amphibole + olivine (ol) + orthopyroxene (opx) + clinopyroxene (cpx) + spinel (spl), one sample contains garnet, and one contains plagioclase. Location selection was purposefully varied in an attempt to capture mantle conditions at different locations as well as potentially capturing different tectonic settings and emplacement mechanisms. Two pyroxene thermometry yields temperatures of 660 to 900°C at pressures (P) ranging from 5.8 – 15 kbar. Estimates of water activities (aH_2O), based on amphibole equilibria, range from 0.07 to 0.4, except for samples from New Caledonia which record values between 0.87 and 1.0. The compositions of co-existing spl + ol + opx yield oxygen fugacities (fO_2) ranging from 0.0 to 1.9 $\Delta\log fO_2$(FMQ).

Low values of aH_2O (< 0.4) are similar to values recorded in other amphibole-bearing peridotites. Amphibole growth in peridotites is often attributed to rock interaction with a metasomatic fluid. This may be the case in some samples, however, the resulting low water

activities suggest that any water present in a metasomatic fluid was likely consumed entirely by the growth of amphibole, resulting in relatively "dry" rocks. However, it is possible that the water needed to stabilize amphiboles present in some of the samples here may have been derived from H present in the co-existing NAMs. Regardless of amphibole formation mechanism it is clear that amphibole bearing peridotites are not necessarily "hydrous" or "wet" as compared to non-amphibole bearing peridotites.

The samples from New Caledonia are the first mantle derived samples to record high values of aH_2O (0.87 -1.0) relative to other studies that have employed similar methods. These are the only samples in this suite that are derived from a paleo oceanic transform fault setting. High values of aH_2O in these rocks are consistent with the idea that fluid may infiltrate oceanic transform faults to depths that corresponding to temperatures between 600 °C and 1100 °C .

Ultimately, these samples provide important insights into fluid conditions at a variety of mantle settings, as well as mechanisms for amphibole growth in mantle peridotites. Additionally, these samples (particularly those that record of high aH_2O) should permit future insight into the amount of H-loss experienced by NAM's during emplacement, and the role of metasomatism in amphibole growth in mantle derived peridotites.

CONTRIBUTORS AND FUNDING SOURCES

Contributors

This work was supported by a thesis committee consisting of Professors William Lamb and Julie Newman of the Department of Geology and Geophysics and Professor Franco Marcantonio of the Department of Oceanography.

Samples were provided by Basil Tikoff and Vasilieos Chatzaras. Additional discussion with V. Chatzaras aided in calculations and interpretations made with respect to samples in this study.

All other work for the thesis was conducted by the student under the advisement of Professor William Lamb of the Department of Geology and Geophysics.

Funding Sources

Graduate study was supported by fellowships from Texas A&M University, Talisman Energy, and Family of Mr. Michel T. Halbouty/American Association of Petroleum Geologists Foundation, the College of Geosciences at Texas A&M University, and the Department of Geology and Geophysics at Texas A&M University.

TABLE OF CONTENTS

Page

LIST OF FIGURES

FIGURE Page

LIST OF TABLES

INTRODUCTION

Water has a significant influence on many physio-chemical properties of upper mantle rocks including viscosity, melting temperature, conductivity and possibly seismic properties (Wyllie, 1971, 1977; Kushiro, Yoder and Mysen, 1976; Karato, 1985; Ranalli, 1995; Karato and Jung, 1998). Several studies have found that incorporating water dependent rheology into global mantle convection models has a strong effect on mantle dynamics (Sandu, Lenardic and McGovern, 2011; Nakagawa, Nakakuki and Iwamori, 2015). Water content and its effects on rheology can have significant controls on mantle cooling history, initiation of plate tectonics, and continental growth (Crowley, Gerault and O'Connell, 2011; Korenaga, 2011; Honing and Spohn, 2016).

Water may also influence the location of phase transitions in pressure-temperature space. This influence may go beyond the stability of hydrous phases such as amphibole and mica. For example, increasing water content in olivine and it's polymorphs can reduce the pressure of the olivine to wadsleyite transition (Wood, 1995; Chen *et al.*, 2002).

The availability of water influences the composition and quantity of liquids derived from partial melting of the mantle, as well as dictating the P-T conditions at which these melts will form (Burnham, 1979; Gaetani and Grove, 1998; Green and Falloon, 1998, 2005). The addition of a melt phase may reduce the viscosity of the mantle. However, partial melting may remove H_2O from mantle minerals effectively increasing the viscosity of the mantle (Hirth and Kohlstedt, 1996). A discontinuity in mantle viscosity can occur due to this extraction of water due to partial melting, and this melting may be responsible for the rheologic differences between lithospheric and asthenospheric mantle (Hirth and Kohlstedt, 1996). Given the potential for water to be an

important factor in mantle dynamics, it is desirable to make accurate estimates of the activity of water within the mantle.

Water is defined here to include H-bearing species present: (1) as a free fluid phase, in which H_2O is one of the dominant H-bearing species, (2) dissolved in melts, (3) or as structurally bound OH and/or H present in minerals. Previous studies have made estimates of mantle water content through measurement of the water present within nominally anhydrous minerals (NAMs) such as olivines, pyroxenes, and garnets (Bell and Rossman, 1992; Ingrin and Skogby, 2000; Beran and Libowitzky, 2006; Skogby, 2006; Peslier *et al.*, 2010, 2017; Demouchy *et al.*, 2015; Demouchy and Bolfan-Casanova, 2016). The water contents of the NAMs in these studies are estimated through the measurement of H, not molecular H_2O, likely present within defects of the crystal structure of these minerals. Experimentally determined diffusion rates of H within NAMs suggests that these minerals are potentially subject to rapid loss of H (Ingrin and Skogby, 2000). These rapid diffusion rates require that extra care be taken when interpreting the significance of measured H content in NAMs, as there may have been H loss during emplacement. Further, the relations between the H contents in many NAMs and H_2O fugacities is poorly understood. The H_2O content in olivine, perhaps the best constrained NAM in terms of this relation, depends not only upon H_2O fugacity (fH_2O) during equilibration, but also upon oxygen fugacity and crystal chemistry (Gaetani *et al.*, 2014). Therefore, it would be desirable to utilize/develop a different proxy for mantle water contents that is devoid of these issues. Ultimately, this would allow for the comparison of mantle water content values obtained using different methods, which may potentially provide insight into the strengths and weaknesses of any particular approach.

Amphibole equilibria can be applied to determine values of aH_2O ($aH_2O = fH_2O/fH_2O^\circ$, where fH_2O° is the fugacity of pure H_2O at the P and T of interest). Areas of the upper mantle may

be infiltrated by metasomatic fluids (e.g. Dawson 1980; Coltorti et al. 1999; Szabó et al. 2004), and amphibole in mantle peridotites is often attributed to formation as a result of metasomatism. Metasomatic fluids may contain H_2O which may help to stabilize amphibole, however, the presence of amphibole does not require H_2O-rich fluids and the most common fluid types may be mantle derived such as basaltic and, perhaps less commonly, carbonatitic melts (Wilshire and Trask, 1971; Tatsumi, 1986, 1989; Agrinier *et al.*, 1993; Coltorti *et al.*, 2004; Liu *et al.*, 2010). Additionally, the presence of amphibole does not require the presence of a lithostatically pressured fluid (volatile) phase, and, in some instances, the H present in NAMs may serve as the source of OH in amphiboles (Kang, Lamb and Drury, 2017).

The primary focus of this study is the application of phase equilibria to gain insight into the nature of mantle fluids. Dehydration equilibria involving a hydrous phase, such as amphibole, is used here to estimate values of mantle water activity, via application of a method similar to that developed by Lamb and Popp (2009). Additionally, values of oxygen fugacity (fO_2) have been determined from spinel equilibria (Wood, 1990). aH_2O estimated with these methods, combined with determinations of P, T, fO_2, and olivine chemistry, allows for the prediction of expected H-content of olivine using experimentally determined relations (Zhao, Ginsberg and Kohlstedt, 2004; Mosenfelder *et al.*, 2006; Gaetani *et al.*, 2014). In future studies we plan to determine expected H-content of olivine and measure H-content values of olivine using Fourier transform infrared spectroscopy. We then plan to compare predicted values of olivine H-content with measured values. This comparison may allow for insights into whether H_2O contents of olivine are truly representative of mantle aH_2O.

GEOLOGIC SETTING

Samples from six different localities were obtained for this study from: Bestiac, France, Lherz, France, Turon de Técouère, France, Almklovdalen, Norway, California, USA and New Caledonia. Sample locality selection was purposefully varied in an attempt to sample mantle conditions at a number of different locations as well as allowing for the potential capture of varying tectonic setting and emplacement mechanisms. A brief summary of the geologic setting of each sample is given below.

French Pyrenees

Samples Bestiac, PL-4, and PTT1 were collected by Basil Tikoff at Bestiac, Lherz, and Turon de Técouère, France respectively. These samples are representative of three of the approximately 40 peridotite bodies that exist in the Pyrenees. A variety of emplacement mechanisms have been proposed for the peridotite bodies of the Pyrenees including both convergent and divergent tectonic processes (Lagabrielle and Bodinier, 2008). Most recent models describe a hyper-extended passive margin that experienced rifting during the separation of the Iberian and European plates, and opening of the Bay of Biscay (Choukroune *et al.*, 1973; Lagabrielle and Bodinier, 2008; de Saint Blanquat *et al.*, 2016). Crustal thinning due to extension allowed for exhumation and denuding of the subcontinental mantle, which in turn allowed for subsequent reworking of peridotites into sediments, and preservation as tectonic lenses (Lagabrielle and Bodinier, 2008; Lagabrielle, Labaume and de Saint Blanquat, 2010; Clerc *et al.*, 2015; de Saint Blanquat *et al.*, 2016). Pyrenean peridotites potentially represent exhumed mantle material from a variety of depths, and mantle material with varied history as evidenced by differences in serpentinization, mineralogy, and evidence of potential exposure to hydrothermal fluids (Bodinier, Dupuy and Dostal, 1988; Fabriès *et al.*, 1989; Le Roux *et al.*, 2007; Lorand, Alard

and Luguet, 2010; de Saint Blanquat *et al.*, 2016; Uenver-Thiele *et al.*, 2017). Recent workers have adopted a dichotomous classification of Pyrenean peridotites (e.g. Lagabrielle *et al.*, 2010; Clerc *et al.*, 2012; de Saint Blanquat *et al.*, 2016): (1) sedimentary "S-type" peridotites which describe peridotite clasts of varying size entrained within Mesozoic meta-sedimentary breccias, and (2) tectonic "T-type" peridotites which describe peridotites that occur as tectonic lenses interpreted to represent mid-cretaceous detachment faults that were inverted during the Late Cretaceous-Cenozoic orogeny (de Saint Blanquat *et al.*, 2016). The samples in this study from Bestiac and Lherz are likely of the "S-type" classification as described by de Staint Blanquat *et al.*, 2016 and Clerc *et al.*, 2012 respectively, while the sample from Turon de Técouère is likely of the "T-type" classification, given the lack of association with Mesozoic breccias (Vissers *et al.*, 1997; Newman *et al.*, 1999). Two recrystallization stages are described in peridotites from the French Pyrenees (Fabries *et al.*, 1991). The first occurring at 900 – 1000 °C and pressures within the stability field of spinel (8-17 kbar), and the second episode occurred between 600 – 750 °C and pressures greater than 8 kbar in eastern massifs such as Lherz, and between 6 - 7 kbar in western massifs such as Turon de Técouère (Fabriès and Conquéré, 1983; Conquéré and Fabriès, 1984; Bodinier, Dupuy and Dostal, 1988; Fabries *et al.*, 1991). Additionally, Newman *et al.*, 1999 estimates that production of matrix minerals occurred between 750 – 850 °C and between 5 – 10 kbar within their peridotite samples from Turon de Técouère.

Almklovdalen, Norway

Sample Almklovdalen was provided by B. Tikoff and collected from the garnet bearing peridotite bodies that are present within the Western Gneiss Region (WGR) of Norway. The WGR is an extension of the Scandinavian Caledonides which evolved during the Caledonian Orogeny, with the closure of the Iapetus sea, and westward subduction of the Baltic Plate beneath Laurentia

(Krogh, 1977; Gee *et al.*, 2008). During the Caledonian Orogeny several series of thin-skinned thrust sheets were emplaced onto the Baltoscandian continental margin. These thrust sheets are organized into five complexes: the autochthon/parautochthon, and uppermost, upper, middle, and lower allochthons, with the peridotite bodies occurring within the autochthon/parautochthon (Medaris, 1984; Gee *et al.*, 2008). These lenses of peridotite and associated metamorphic rocks are argued to have originated at depths in excess of 185 km (van Roermund and Drury, 1998). An uplift P-T pathway for peridotites from the WGR was developed by Spengler *et al.*, 2009 with an upper P-T of ~65 kbar and ~900 °C, peridotites analyzed from this region tend to record P-T conditions that fall along this uplift pathway (e.g. Kang, Lamb and Drury, 2017). Peridotites in the WGR display evidence for varied histories with increasing serpentinization towards the contact between peridotites and surrounding metamorphic rocks, additionally, evidence for hydrothermal interaction is variable with some peridotites containing abundant hydrous phases such as phlogopite, chlorite, and amphibole with other peridotite bodies lacking any such phases (Brueckner and Medaris, 1998; Taylor, 1998; Kostenko *et al.*, 2002; Beyer, Griffin and O'Reilly, 2006). Finally, these peridotites have potentially been subjected to complex metamorphic histories with eight different metamorphic stages having been described by Carswell and van Roermund, 2003.

California, USA

Sample CATRINITY was provided by B. Tikoff and collected from the Trinity Ophiolite Complex in Northern California, USA. The Trinity Ophiolite Complex is a 2-4 km thick eastward dipping sheet that overlies a less dense basement (LaFehr, 1966; Fuis *et al.*, 1987). Several models for the generation of the Trinity Ophiolite exist including formation as a mantle diapir, oceanic lithosphere generated at a mid-oceanic ridge, oceanic crust associated with a backarc-basin setting,

forearc oceanic lithosphere, and volcanic arc basement (Wallin and Metcalf, 1998 and references therein). Recent publications tend to favor the interpretation that the formation of the Trinity Ophiolite is the result of rifting within a back arc basin setting proximal to a subduction zone (Wallin and Metcalf, 1998; Ceuleneer and Le Sueur, 2008; Dygert, Liang and Kelemen, 2016). During the Devonian the Trinity Ophiolite Complex was thrust westward onto the Central Metamorphic Belt which it presently overlies (Lipman, 1964). The peridotites in the Trinity Ophiolite vary in mineralogy and in some instances these mineralogic differences, along with variations in trace elements in clinopyroxene, are thought to record varying degrees of exposure and reaction with ascending basaltic melts (Quick, 1981, 1982; Kelemen, Dick and Quick, 1992; Dygert, Liang and Kelemen, 2016). Studies such as Quick, 1981, and 1982 suggest peridotites from the Trinity ophiolite likely ascended from depths of 60 – 100 km as evidenced by opx core compositions which record temperatures of 1,159 – 1,274 °C and textural evidence suggesting partial melting. Quick, 1981 suggests minerals in these peridotites then re-equilibrated at lower pressures (< 5 kbar) and temperatures ranging from 963 – 1097 °C as recorded by rim compositions of pyroxenes.

New Caledonia

Samples KA04-17A1, BG02-4B1A, BG02-7A1B, and BG04-13A1A were provided by Vasileios Chatzaras and were collected from the New Caledonia Ophiolite, specifically from the Bogota Peninsula shear zone. The basement rocks of New Caledonia are an exposure of the Northfolk Ridge and thought to represent a microcontinental ribbon that rifted from Gondwanaland during the Late-Cretaceous (Dubois, Launay and Recy, 1974; Cluzel, Aitchison and Picard, 2001; Crawford, Meffre and Symonds, 2003). After this period of rifting that separated the Northfolk Ridge from Gondwanaland, a period of convergence and subduction began (Eissen

et al., 1998; Cluzel, Aitchison and Picard, 2001; Crawford, Meffre and Symonds, 2003; Cluzel *et al.*, 2006). During this period of convergence several thrust sheets were emplaced on New Caledonia, including sheets of metamorphosed oceanic crust, accreted forearc material, and the ophiolite nappe of interest (Collot *et al.*, 1987; Cluzel, Aitchison and Picard, 2001). The peridotites exposed on the Bogota Peninsula have been interpreted to represent a N-S striking, dextral paleo-transform fault, which caused the severe deformation present within our samples (Prinzhofer and Nicolas, 1980; Nicolas, 1989; Titus *et al.*, 2011). Pirard, Hermann and O'neill, 2013 report temperatures in the nearby peridotite body Massif du Sud between 795 – 983 °C and pressures less than 13 kbar are inferred due to the lack of garnet.

ANALYTICAL PROCEDURE

The chemical composition of minerals in each sample was characterized using the Cameca SX5 electron microprobe located at Texas A&M University. Olivine, pyroxene, spinel, and garnet were analyzed using an accelerating voltage of 15 kV, an electron beam current of 20nA, and the diameter of the electron beam at the sample (spot size) was 3 μm. Amphiboles were also analyzed using an accelerating voltage of 15kV, but with a spot size of 10 μm and a beam current of 10nA.

Olivine, pyroxene, garnet, plagioclase, and spinel were normalized to 3, 4, 8, 5, and 3 cations, respectively. Amphibole normalization is not as straight forward as the other phases analyzed in this study because it requires the quantification of 3 variables: (1) ratio of $Fe^{3+}$to Fe^{2+}, (2) the amount of oxy-substitution, and (3) proportion of the A-site that is vacant. A complete discussion of the amphibole normalization procedure used in this study can be found in the appendix of Lamb and Popp, 2009, what follows is a brief summary.

Ultimately, we plan to determine $Fe^{3+}/(Fe^{3+} + Fe^{2+})$ with the electron microprobe by applying the method outlined by Lamb *et al.*, 2012. In this method the electron microprobe is used to determine the position of the Fe Lα peak, which changes as a function of $Fe^{3+}/(Fe^{3+} + Fe^{2+})$. To employ this method the Cameca SX5 microprobe at Texas A&M University must be calibrated using amphibole standards with known $Fe^{3+}/(Fe^{3+} + Fe^{2+})$ (which we currently possess from the study of Lamb *et al.*, 2012). At the time of this writing the above-mentioned calibration is ongoing. In the absence of this calibration, or if our amphiboles are not well-suited to the method, the following approach will be utilized. In this case, we assume a value of $Fe^{3+}/(Fe^{3+} + Fe^{2+}) = 0$ or as small as possible to achieve a mineral formula that satisfies charge balance. Minimizing the value of $Fe^{3+}/(Fe^{3+} + Fe^{2+})$ maximizes the OH content within the calculated amphibole formula.

Given a value for $Fe^{3+}/(Fe^{3+} + Fe^{2+})$, the oxy-component of the amphibole is determined by combining this value ($Fe^{3+}/(Fe^{3+} + Fe^{2+})$) with the major and minor element content, and the definition of Z-site occupancy: Z = 2 = OH + F + Cl + O. For mantle amphiboles the amount of oxy substitution can be estimated via two different relations. The first is described by Popp *et al.*, 1995 and equates the amount of O^{2-} in the Z-site to the sum of Fe and Ti in the amphibole:

$$2.0 = Fe^{3+} + Ti^{4+} + OH^{-} + Cl^{-} + F^{-} \qquad (1)$$

This equation requires that $O = Fe^{3+} + Ti^{4+}$. The second relationship is described by King *et al.*, 1999 and is based on the equation:

$$Fe^{3+} = 2.47 - 0.93(OH) - \left(Ti + Al^{Vi}\right) \quad (2)$$

Both these equations are based on analyses of natural amphiboles that originated in the earth's mantle, and the amounts of cations and anions are input as atoms per formula unit (apfu).

Given a value for $Fe^{3+}/(Fe^{3+} + Fe^{2+})$, and the amount of oxy substitution estimated from either equation (1) or (2), the A-site vacancy is estimated through an iterative process that changes the amount of A-site vacancy by extremely small increments until the resulting amphibole formula is charge balanced.

Values of oxygen fugacity (fO_2) were determined using the the oxy-barometers of Wood, 1990 and Miller, Holland and Gibson, 2016. These oxy-barometers are particularly sensitive to accurate quantification of Fe^{3+}/Fe_{Total} in spinel which may be determined from electron microprobe analyses via charge balance. Although sufficiently precise, systematic uncertainties in these spinel analyses (Wood and Virgo, 1989) may yield relatively large uncertainties in Fe^{3+}/Fe_{total}, when estimated from charge balance. Thus, we have applied a method similar to that of Wood and Virgo, 1989 by also analyzing a set of secondary spinel standards with Fe^{3+}/Fe_{total} measured by

Mossbauer spectroscopy (provided by B. Wood). To use these secondary standards to correct EMP measured Fe^{3+}/Fe_{total} values a linear function will be fit between Fe^{3+}/Fe_{total} values calculated for these standards via normalization, and Fe^{3+}/Fe_{total} values measured via Mossbauer. This function will then be applied to spinel unknowns to correct Fe^{3+}/Fe_{total} values calculated by normalization.

SAMPLE DESCRIPTION

French Pyrenees

Samples Bestiac, PL-4, and PTT1 were collected from Bestiac, Lherz, and Turon de Técouère, France respectively. All three samples contain olivine (ol), clinopyroxene (cpx), orthopyroxene (opx), spinel (sp), and amphibole, and can be classified as spinel lherzolites. Sample PTT1 is a protomylonite with a strong foliation, and has large porphyroclasts of cpx, opx, ol, and sp amongst a very fine grain matrix (Figure 1a). Amphibole largely occurs as individual grains amongst the fine grain matrix, near, and possibly replacing, pyroxenes, and as porphyroclasts that are somewhat smaller than other porphyroclasts present within the sample (Figure 1b). Sample PL-4 is foliated and exhibits evidence of deformation via grain size reduction throughout the thin section. Amphibole in PL-4 typically occurs near, and possibly replacing, pyroxenes (Figure 2). Sample Bestiac is also foliated with bimodal grainsizes containing populations of coarse and medium grained ol, opx, cpx, and sp, with amphibole in Bestiac typically occurring near, and possibly replacing, pyroxenes (Figure 3). Grainsize reduction is less severe in Bestiac relative to the other samples from the Pyrenees, with the finer grained population being coarser and less abundant than other samples, suggesting limited deformation relative to other samples.

Almklovdalen, Norway

Sample Almklovdalen collected from the Western Gneiss Region (WGR) of Norway near Almklovdalen, Norway. Almklovdalen is a garnet lherzolite containing olivine, clinopyroxene, orthopyroxene, spinel, amphibole, serpentine and garnet. Garnet exists as large porphyroblasts with kelyphite textures along the rims amongst a finer grain matrix of roughly equal sized ol, opx, cpx, sp, and amphibole. Amphibole is present as individual grains that are similar in size to other minerals in the matrix, and it also occurs as part of the kelyphite rimming the garnets (Figure 4).

Serpentine is pervasive along the grain boundaries of all minerals in the sample. The garnet porphyoblasts were typically devoid of major inclusions with the exception of a few grains which contained orthopyroxene inclusions.

California, USA

Sample CATRINITY was collected from the Trinity Ophiolite Complex in Northern California, USA. CATRINITY is weakly foliated and contains olivine, clinopyroxene, orthopyroxene, spinel, amphibole, plagioclase (plag), and serpentine and is a spinel-plagioclase lherzolite. CATRINITY is moderately fractured with serpentine present in many fractures. Opx and cpx exist as larger porphyroclasts amongst slightly finer grain ol, and sp, amphibole is largely present near, and possibly replacing, pyroxenes (Figure 5).

New Caledonia

Samples KA04-17A1, BG02-4B1A, BG02-7A1B, and BG04-13A1A were collected from the New Caledonia Ophiolite, specifically from the Bogota Peninsula shear zone. These samples are strongly deformed, contain olivine, clinopyroxene, orthopyroxene, spinel, amphibole, and can be classified as spinel harzburgites. These samples all contained large porphyroclasts of opx, and occasional porphyroclasts of spinel amongst a fine grain matrix largely composed of olivine. Lesser amounts of amphibole and clinopyroxene occurred as individual grains, and as intergrown with one another and possible replacing opx (Figure 6). These samples contain large amounts of serpentine indicating the introduction of H_2O-bearing (H_2O-rich?) fluids.

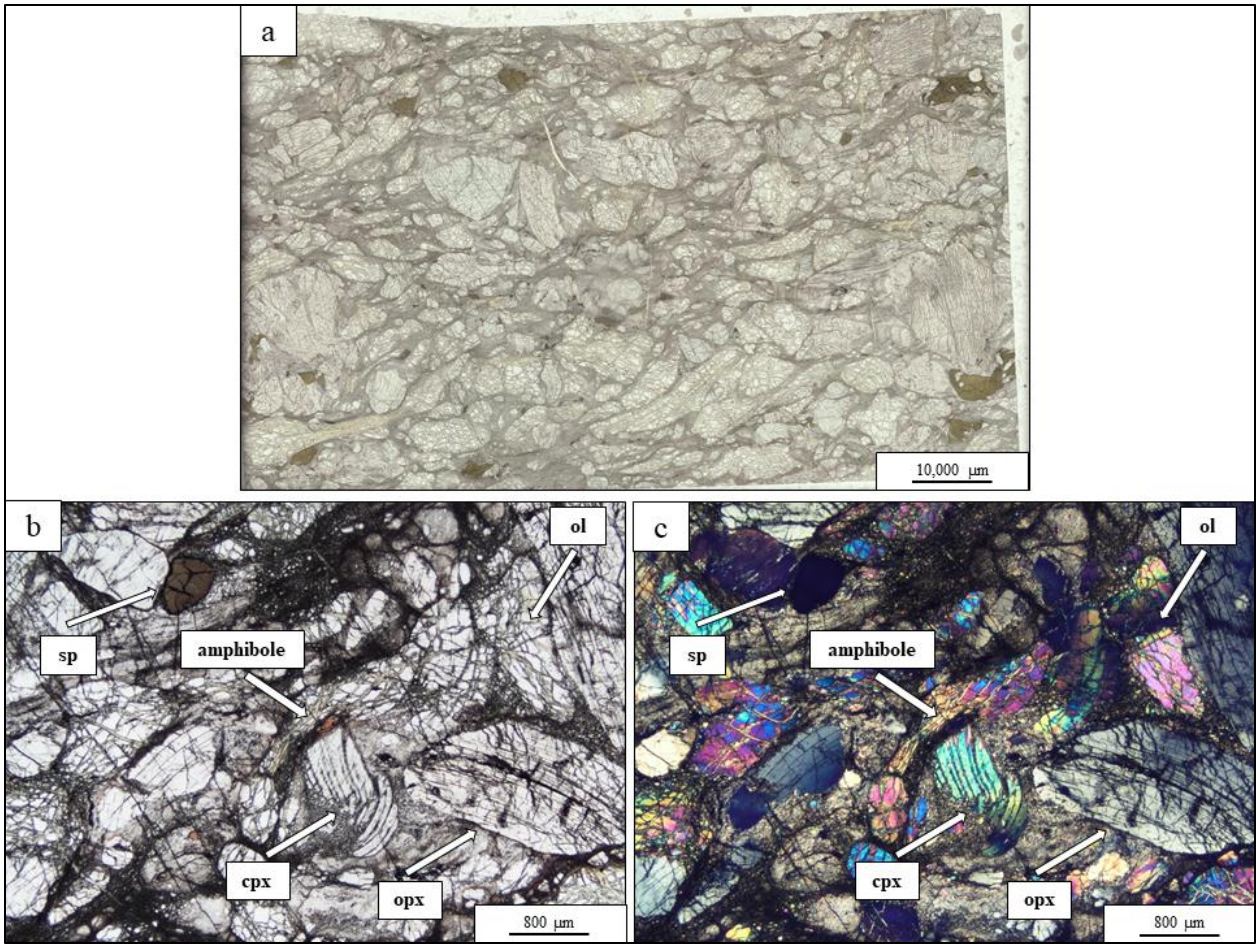

Figure 1. Photomicrographs of sample PTT1: (a) Plane polarized light image of entire PTT1 thin-section showing porphyroclasts amongst a finer grain matrix and foliation present (b) Plane polarized light image showing grain size distribution and amphibole growth texture (c) Cross polarized light image of (b).

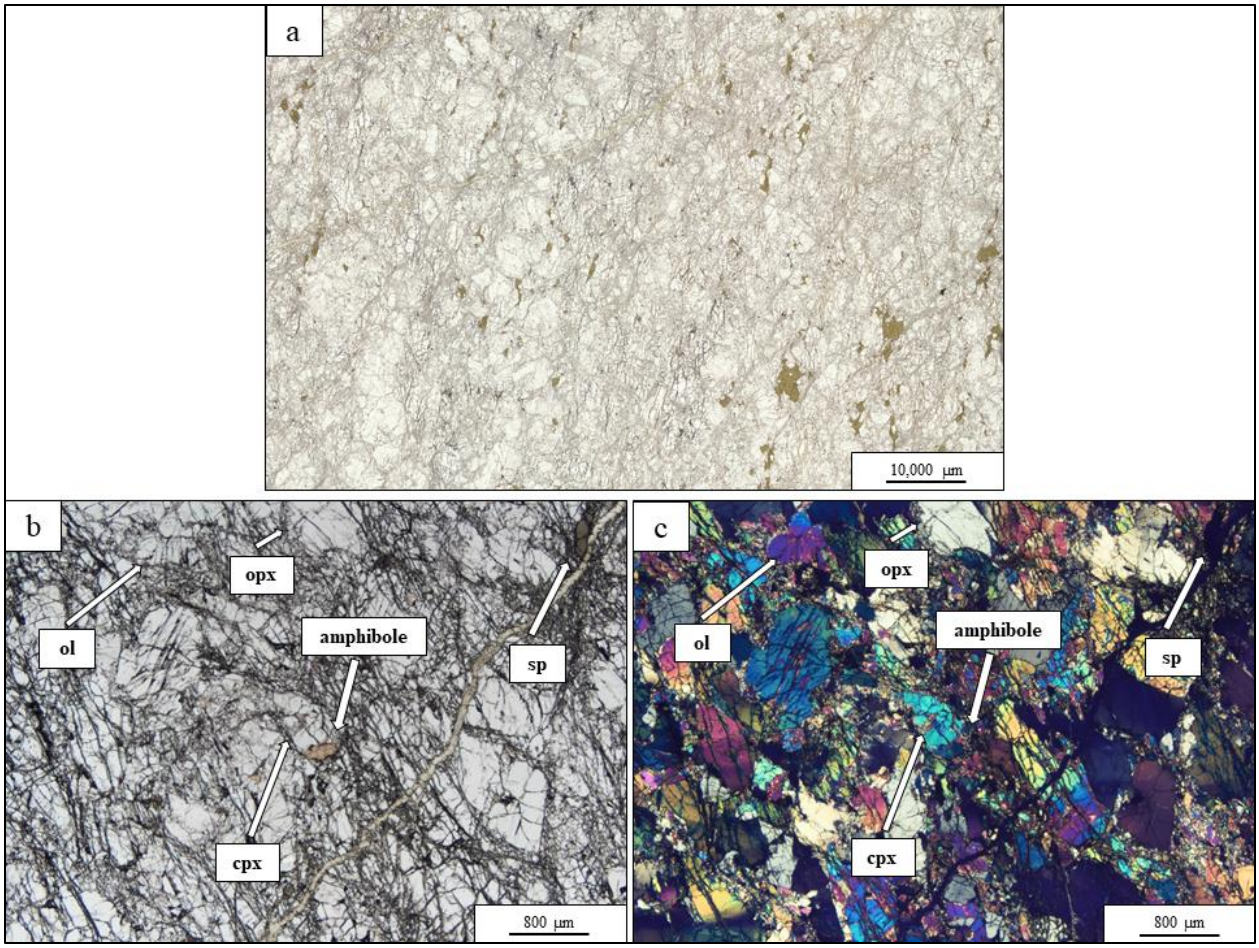

Figure 2. Photomicrographs of sample PL-4 (a) Plane polarized light image of entire PL-4 thin-section showing bands of highly deformed finer-grained material and bands of larger grains (porphyroclasts) (b) Plane polarized light image showing grain size distribution and amphibole growth texture (c) Cross polarized light image of (b).

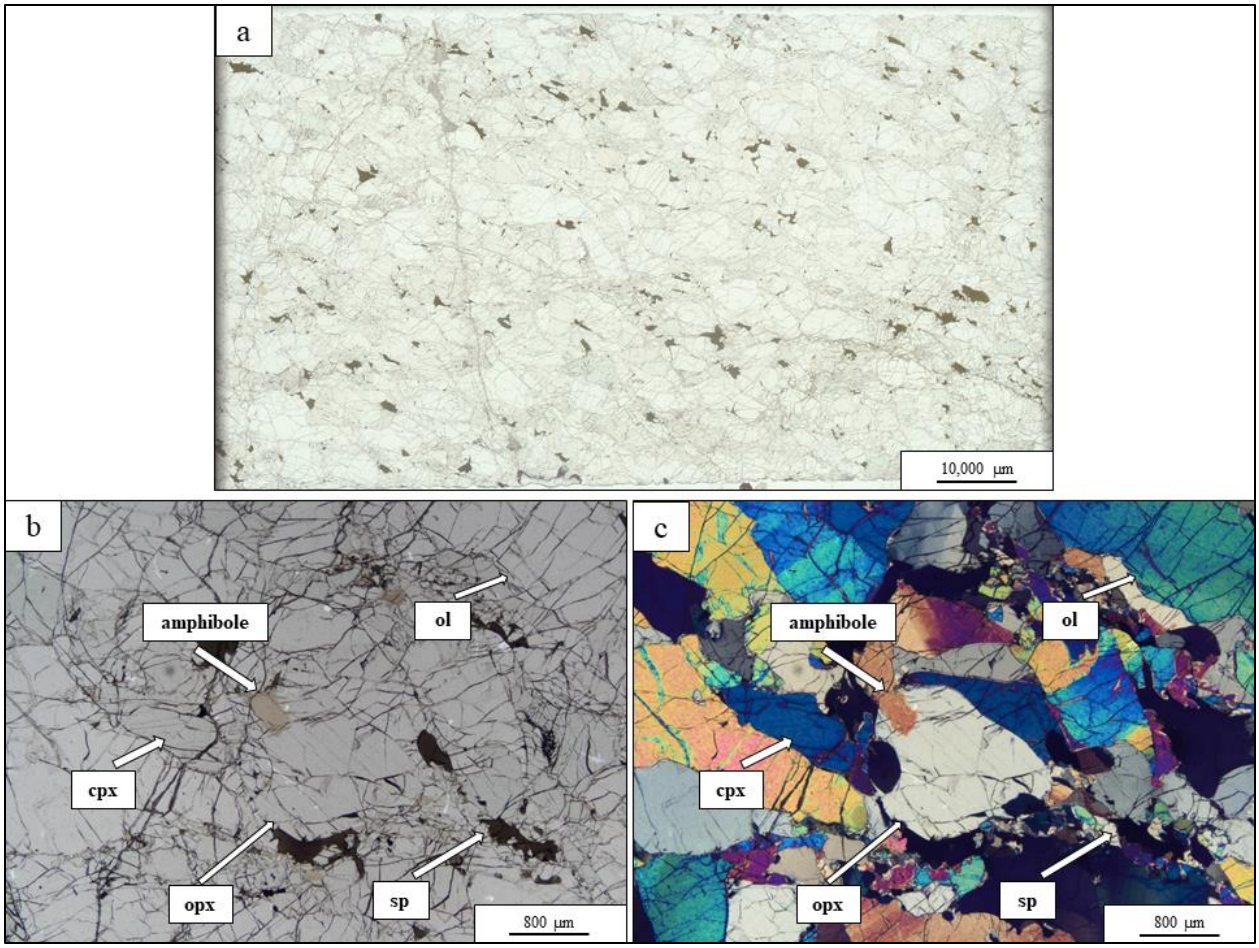

Figure 3. Photomicrographs of sample Bestiac (a) Plane polarized light image of entire Bestiac thin-section showing bimodal grain size distribution (b) Plane polarized light image showing grain size distribution and amphibole growth texture (c) Cross polarized light image of (b).

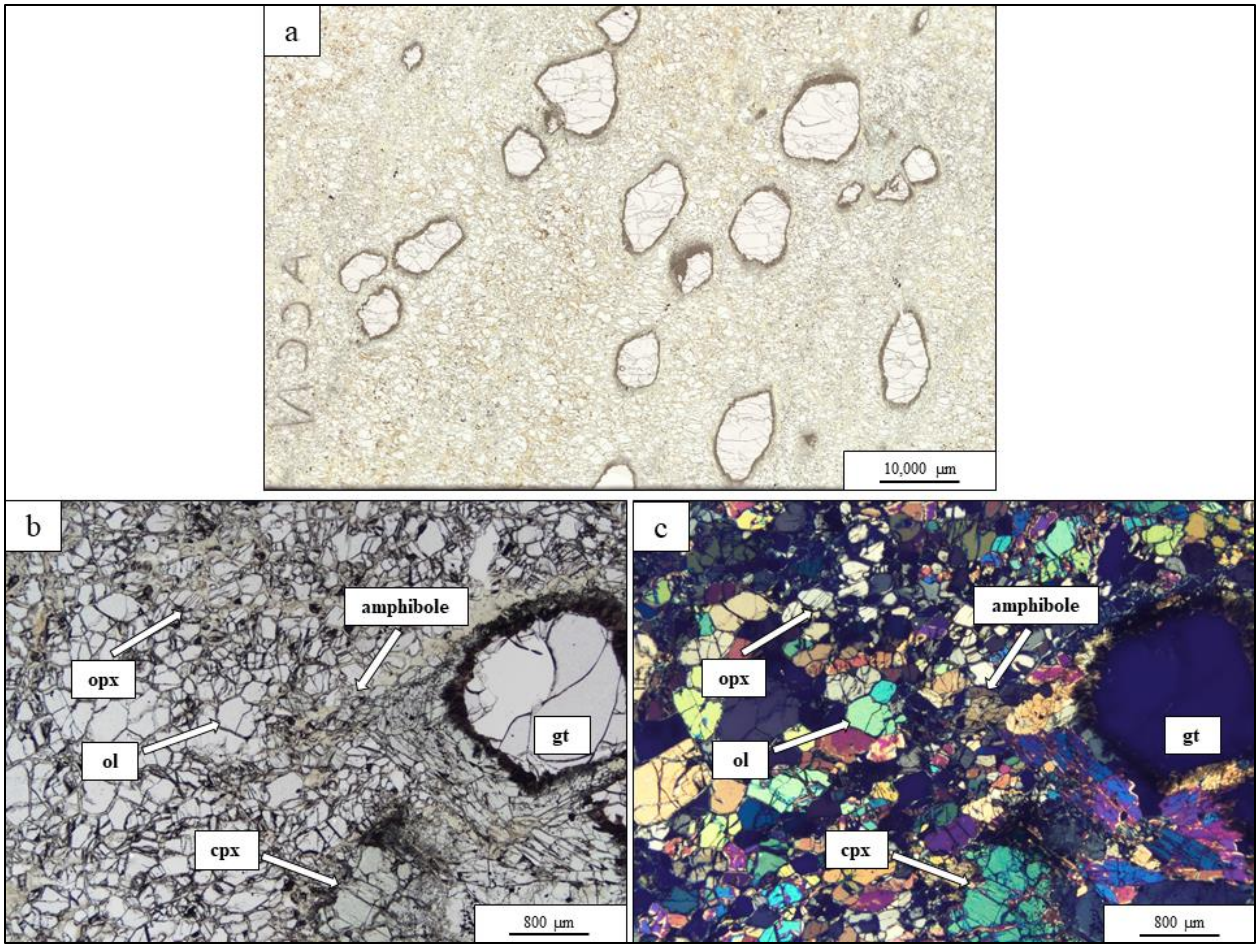

Figure 4. Photmicrographs of sample Almklovdalen (a) Plane polarized light image of entire Almklovdalen thin-section showing large garnet porphyroblasts amongst a finer grain matrix of other phases (b) Plane polarized light image showing grain size distribution and amphibole growth texture along with kelyphite texture along garnet rim (c) Cross polarized light image of (b).

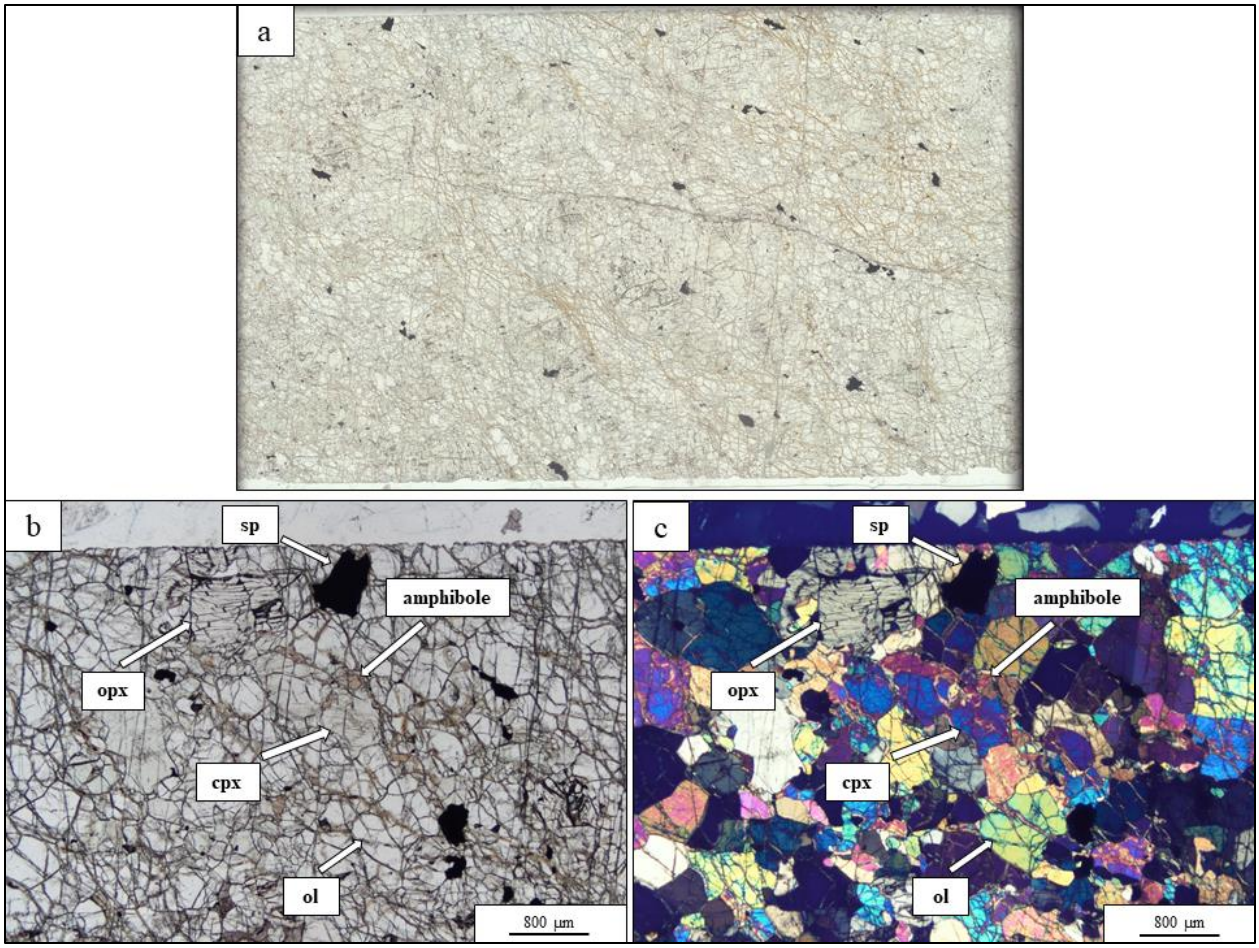

Figure 5. Photomicrographs of sample CATRINITY (a) Plane polarized light image of entire CATRINITY thin-section showing slightly larger pyroxene porphyroblasts amongst smaller ol, sp, plag, and amphibole (b) Plane polarized light image showing grain size distribution and amphibole growth texture (plag absent in photo) (c) Cross polarized light image of (b).

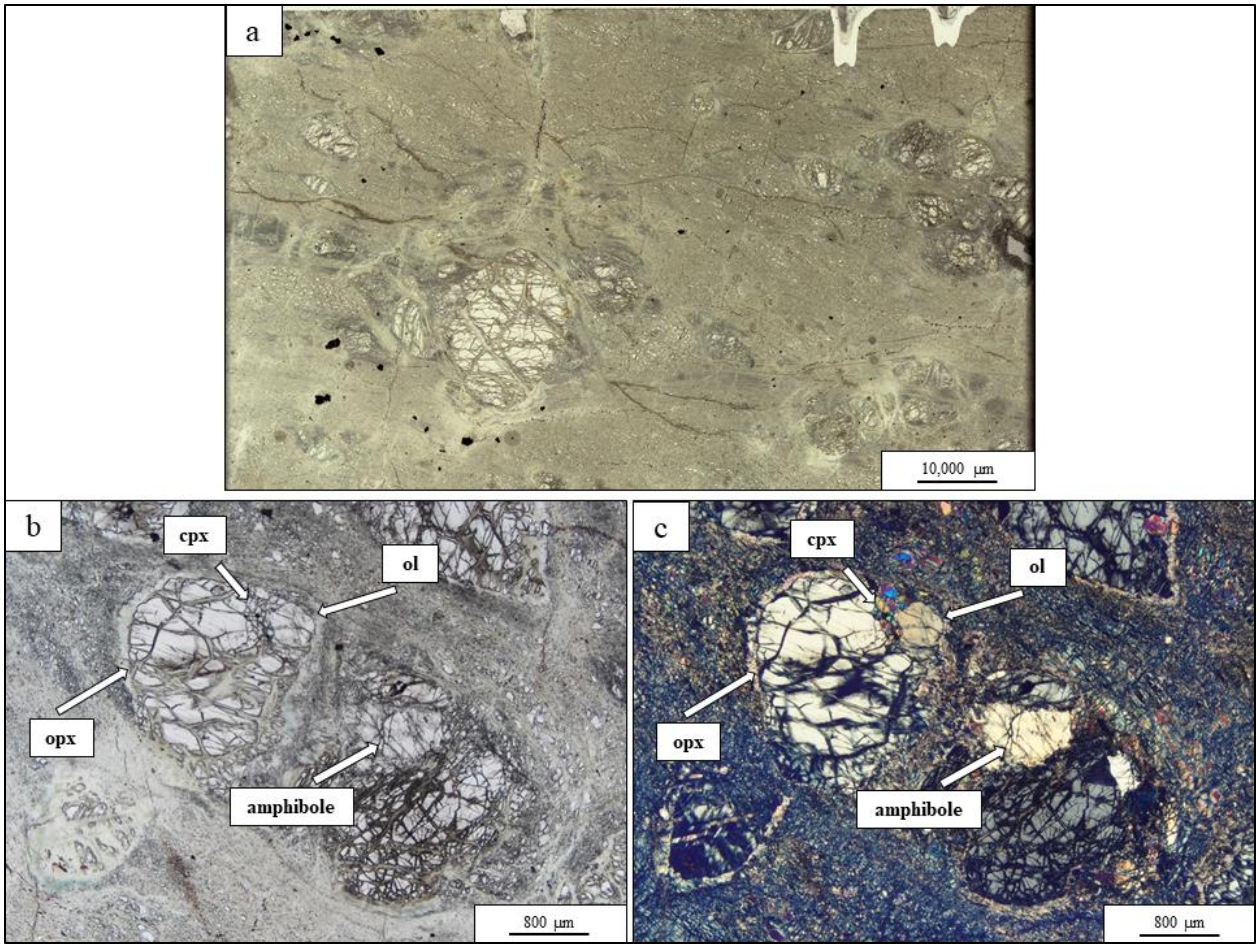

Figure 6. Photomicrographs of sample KA04-17A1 (a) Plane polarized light image of entire KA04-17A1 thin-section showing large orothopyroxene porphyroblasts amongst fine grain matrix of olivine, spinel, and serpentine (b) Plane polarized light image showing grain size distribution and amphibole growth texture (spinel absent in photo) (c) Cross polarized light image of (b).

MINERAL CHEMISTRY

Observable general trends in each phase are discussed below. Figures accompanying this section show data from individual grains that are used as representative examples for their respective samples. Data from mineral analyses of sample KA04-17A1 are used as a representative example for the three other New Caledonia samples.

Olivine

Mg #s (Mg/Mg+Fe) for olivine range from 0.89 – 0.92 for all samples. Olivine chemistry was homogenous core to rim across individual olivine grains, as well as homogenous with respect to other olivine grains within samples.

Clinopyroxene

Clinopyroxene Mg #s range from 0.88 – 0.95 for all samples, Fe^{3+}/Fe_{total} calculated via charge balance ranges from 0.0 – 1.0. Most grains lack pronounced concentric zoning, however slight concentric and non-concentric zoning can be observed in porphyroclasts and matrix grains from some samples. In sample PTT1 Ca and Mg increase slightly from core to rim, while Al decreases (Figure 7a). PL-4 displays non-concentric zoning with higher Al, and lower Ca, Mg, and Si towards one rim (Figure 7b). In Almklovdalen Ca and Mg increase core to rim with slight Al decrease core to rim (Figure 7d). Samples KA04-17A1, Bestiac, and CATRINITY do not display obvious compositional zoning (Figure 7c, 7e,7f).

Orthopyroxene

Orthopyroxene Mg #'s range from 0.89 – 0.93 for all samples, Fe^{3+}/Fe_{total} calculated via charge balance ranges from 0.0 – 0.40. Most grains are slightly concentrically zoned with decreasing Ca and Al core to rim and increasing Si and Mg (Figure 8).

Amphibole

Zonation in amphibole is difficult to discern in these samples, a slight concentric zonation exists within some samples with the general trend being decreasing Si, Mg, and Ca core to rim and increasing Al and Fe (Figure 9).

Spinel

Mg #s in Spinel range from 0.37 – 0.75 for all samples, Fe^{3+}/Fe_{total} calculated via charge balance and then corrected using methods described above range from 0.0 – 0.30. Zoning is difficult to discern in samples PL-4 and Bestiac (Figure 10b, 10c), concentric zoning exists in samples PTT1 and CATRINITY with decreasing Al and increasing Cr and Fe from core to rim (Figure 10a, 10e). The sample from Almklovdalen exhibits decreasing Cr and Fe from core to rim with increasing Al and Mg (Figure 10d). Sample KA04-17A1 shows decreasing Cr and Mg core to rim with increasing Fe and Al (Figure 10f).

Garnet and Plagioclase

Garnets in sample Almklovdalen and plagioclases in sample CATRINITY are relatively homogenous and lack concentric zoning.

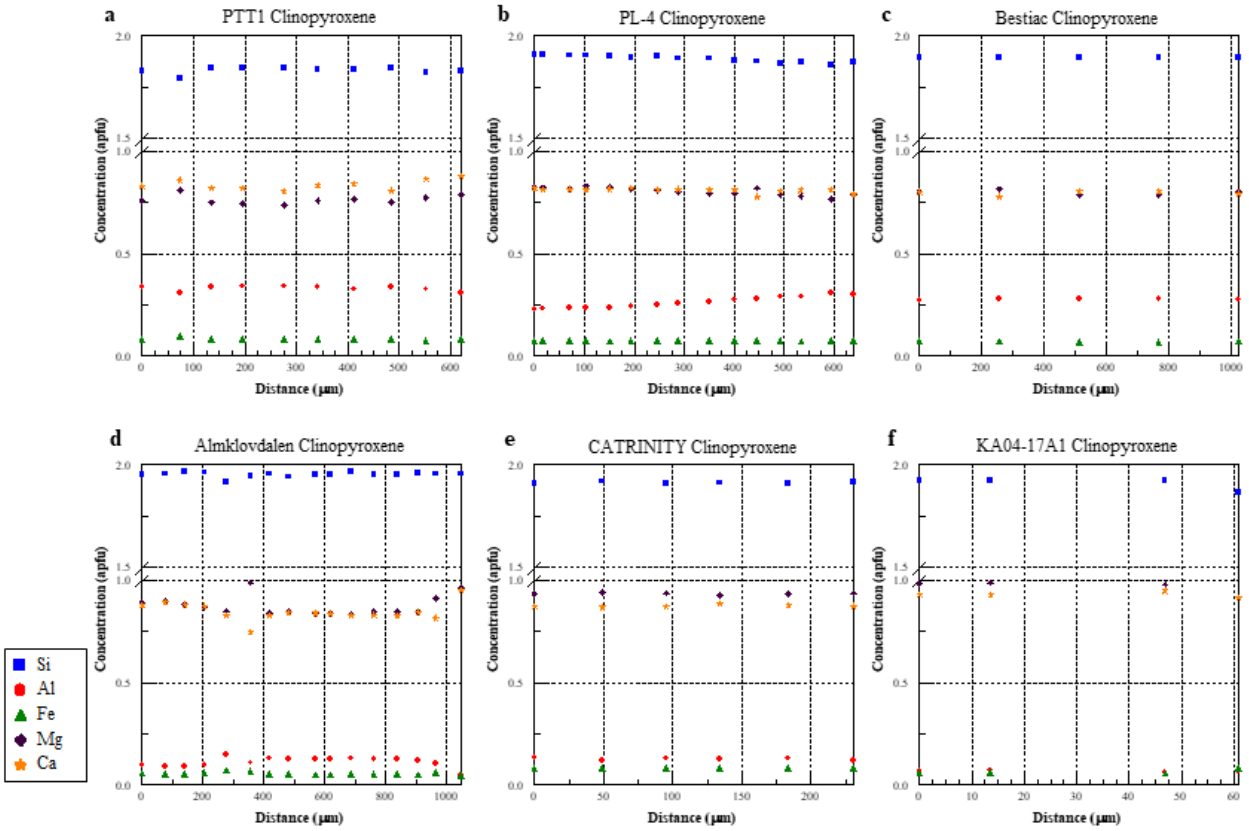

Figure 7. Chemical analyses from EPMA on clinopyroxene grain in samples (a) PTT1 (b) PL-4 (c) Bestiac (d) Almklovdalen (e) CATRINITY (f) KA04-17A1. Analysis represent traverses from rim to core to rim across an individual grain.

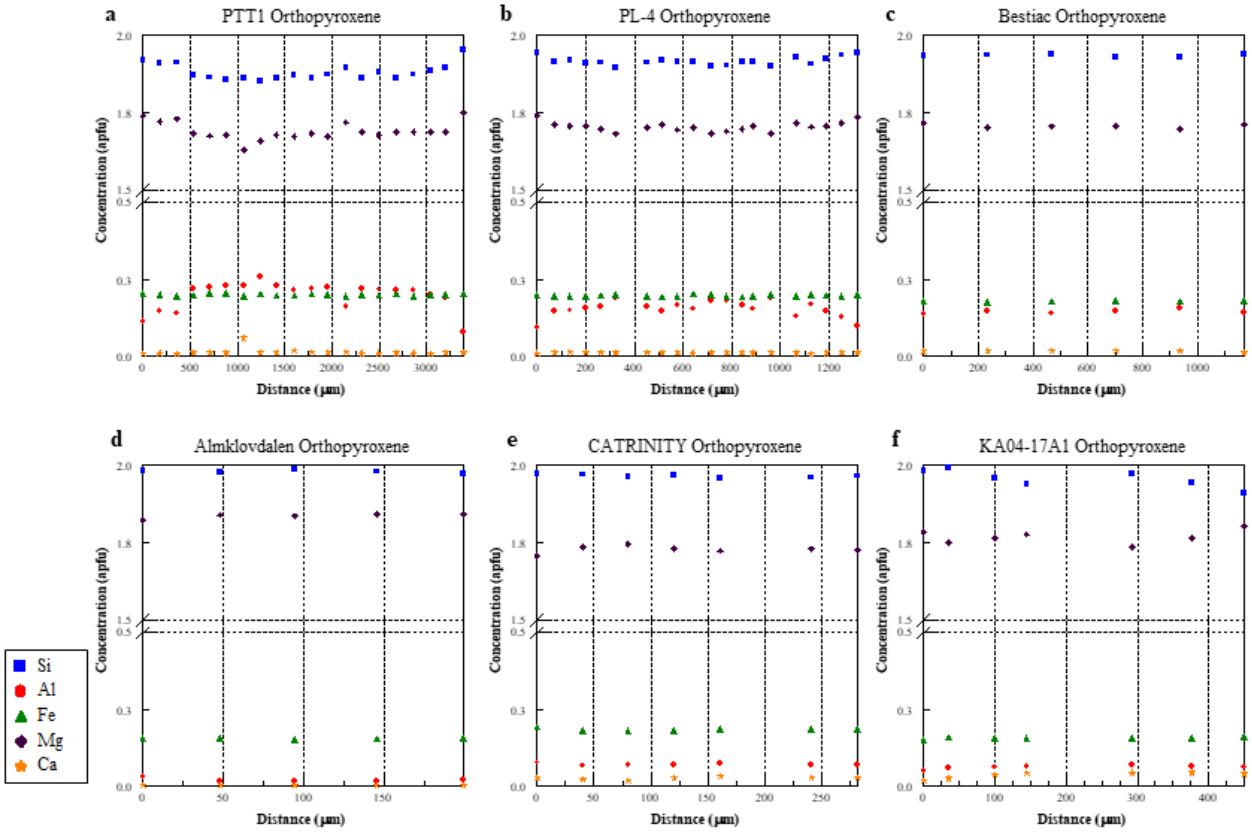

Figure 8. Chemical analyses from EPMA on orthopyroxene grain in samples (a) PTT1 (b) PL-4 (c) Bestiac (d) Almklovdalen (e) CATRINITY (f) KA04-17A1. Analysis represent traverses from rim to core to rim across an individual grain.

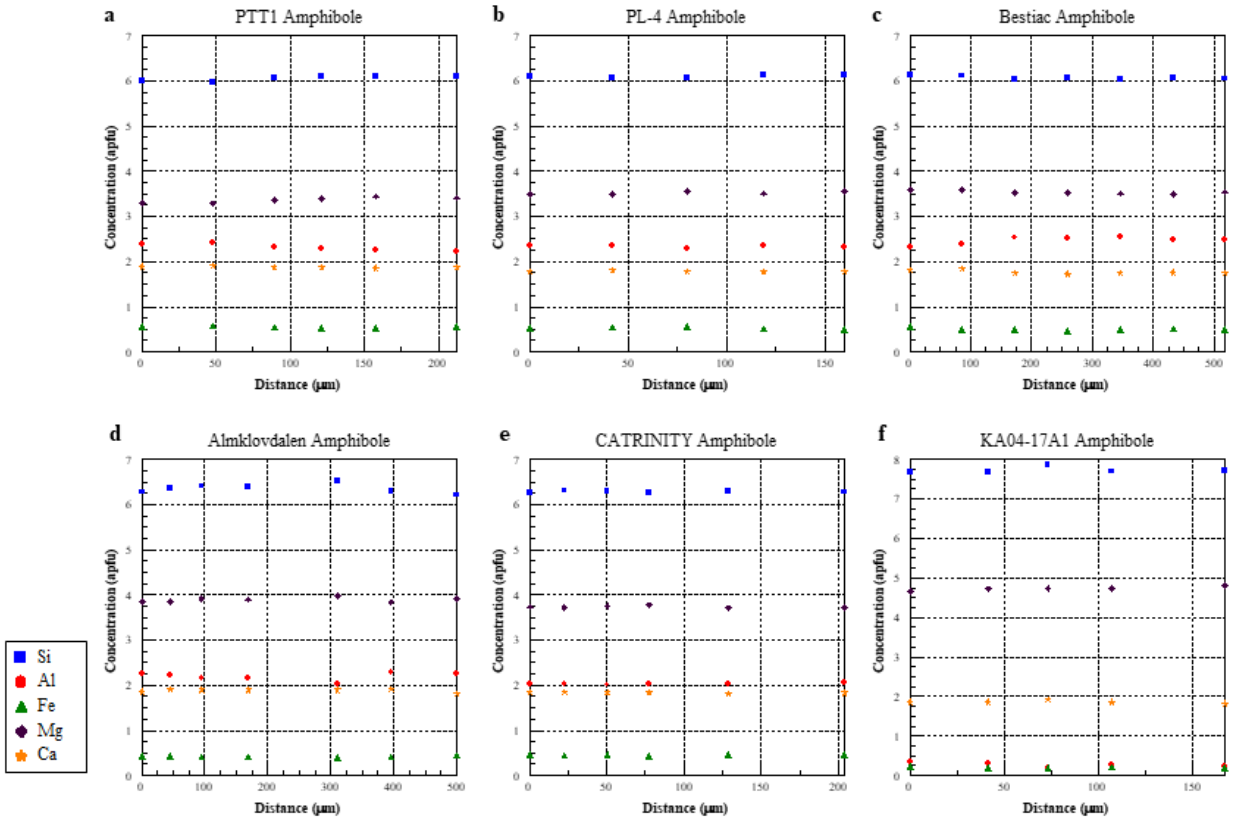

Figure 9. Chemical analyses from EPMA on amphibole grain in samples (a) PTT1 (b) PL-4 (c) Bestiac (d) Almklovdalen (e) CATRINITY (f) KA04-17A1. Analysis represent traverses from rim to core to rim across an individual grain.

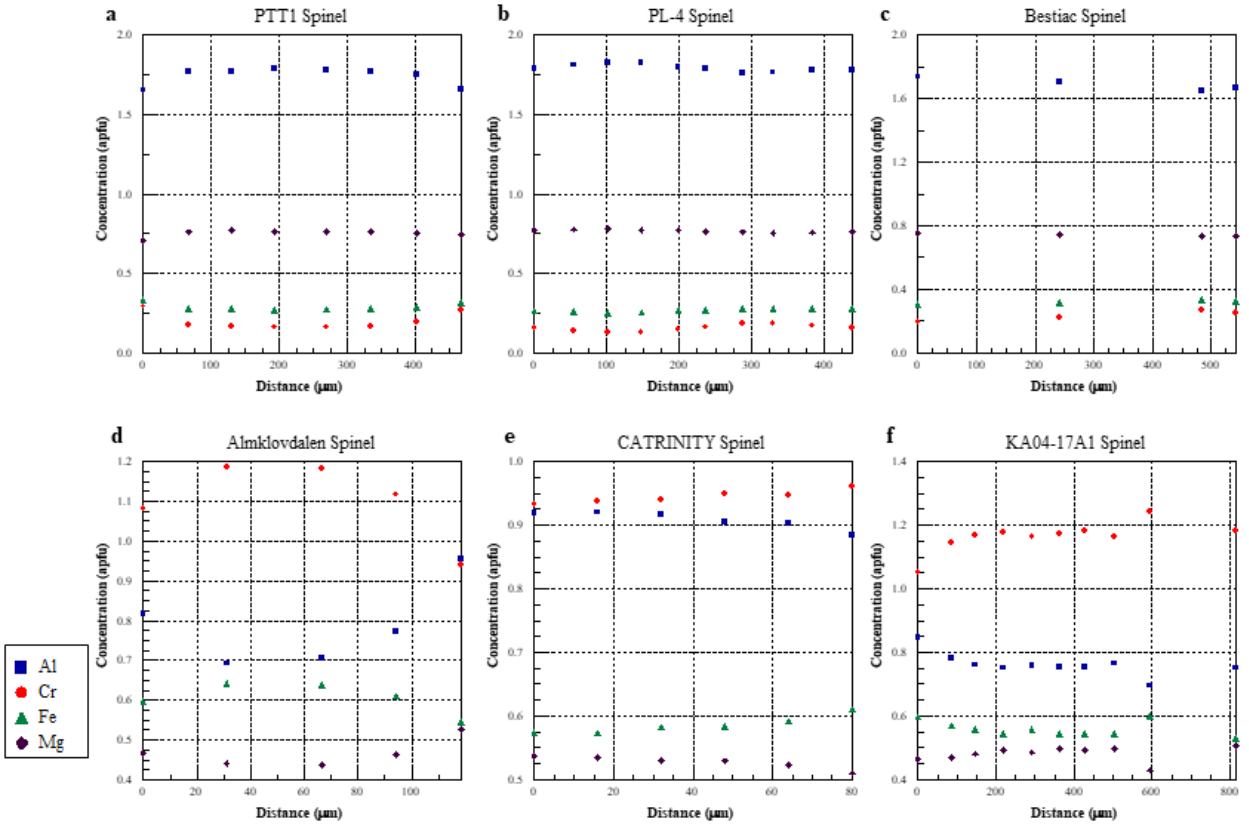

Figure 10. Chemical analyses from EPMA on spinel grain in samples (a) PTT1 (b) PL-4 (c) Bestiac (d) Almklovdalen (e) CATRINITY (f) KA04-17A1. Analysis represent traverses from rim to core to rim across an individual grain.

TEMPERATURE AND PRESSURE

The primary goal of this study is to utilize various equilibria to estimate the fugacities of fluids recorded by mineral equilibria. Estimating values of aH_2O ($aH_2O = fH_2O/fH2O^\circ$ where fH_2O° is the fugacity of pure H_2O at the P and T of mineral equilibration) and $fO2$ using mineral equilibria requires an independent determination of pressure and temperature. Temperatures of mineral equilibration can be determine by application of conventional geo-thermometry, and many thermometers applicable to mantle peridotites have been formulated (O'Neill and Wood, 1979; Brey and Köhler, 1990; Taylor, 1998; Xu, Lin and Shi, 1999; Nimis and Taylor, 2000; Nimis and Trommsdorff, 2001; Wu and Zhao, 2007; Nimis and Grütter, 2010). Of these geo-thermometers, the two-pyroxene thermometer of Taylor and Green, 1988 consistently reproduces experimental temperatures in peridotites of various compositions (Nimis and Grütter, 2010) and, therefore, is the geo-thermometer used in this study.

The pressure of mineral equilibration for the one garnet-bearing peridotite (sample Almklovdalen) examined in this study was determined using the Al-in-OPX geo-barometer of Nickel and Green, 1985. This choice of geo-barometer was based on the work of Nimis and Grütter, 2010, who argue that the Nickel and Green, 1985 can more accurately reproduce pressures of experiments performed on peridotites as compared to other formulations of this geobarometer.

Sample CATRINITY contained both plagioclase and spinel and as such the following equilibria could be written:

$$2\,Fo + An \leftrightarrows En + Di + Sp \qquad (3)$$

Equilibria (3) involves the following end-members in natural phases: forsterite ($Fo = Mg_2SiO_4$) in olivine, anorthite ($An = CaAl2Si2O8$) in plagioclase, enstatite ($En = MgSiO_3$) in orthopyroxene, diopside ($Di = CaMgSi_2O_6$) in clinopyroxene, and spinel ($Sp = MgAl_2O_4$). The location of

equilibria (3) in P-T space can be determined using the THERMOCALC software of Holland and Powell, 2011 in conjunction with determined mineral end-member activities (a full discussion of the determination of end-member activities follows in a later section of this thesis).

Many of the samples in this study contain spinel and lack garnet or plagioclase. As noted by MacGregor, 2015, a reliable geobarometer for spinel-bearing peridotites has not been calibrated. Köhler and Brey, 1990 developed a geothermobarometer based on the Ca exchange between clinopyroxene and olivine. However, as noted by workers such as Smith, 1999 this method has seen limited application due to difficulty in measuring trace quantities of Ca in olivine, rapid diffusion of Ca in olivine, and the methods sensitivity of the pressure determination to temperature. The range of pressures over which spinel is stable in a peridotite containing both cpx and opx, is limited by a reaction that produces plagioclase at low P (equilibria 3 above) and garnet at high P. Experimental studies in the CaO-MgO-Al_2O_3 system have determined that at 900˚C spinel stability ranges from ≈9 kbar to ≈15 kbar (Jenkins and Newton, 1979; Gasparik, 2000; Klemme and O'Neill, 2000). However, other components are common in spinel-bearing peridotites, including Cr, and Fe, and these components may extend the stability of spinel. It has been argued that spinel, in peridotites with compositions typically found in the upper mantle, is stable from approximately 10 to 20 kbar and, therefore, 15 kbar may be taken as a reasonable estimate of the pressure of mineral equilibration (Mori, 1977; Woodland, Kornprobst and Wood, 1992; Lamb and Popp, 2009; Nkouandou and Temdjim, 2011).

For all samples in this study a lower and upper pressure spinel stability limit was calculated using THERMOCALC software (Holland and Powell, 2011) to determine reaction locations (in P-T space) for the reaction from anorthite- to spinel-bearing peridotite and the reaction from spinel- to pyrope-bearing peridotite, respectively. To determine the lower pressure spinel stability limit

from equilibria (3), an activity of unity was assumed for anorthite (with the exception of plagioclase bearing samples where the calculated activity of anorthite was used), and the calculated activity for other mineral endmembers was used (see later section for endmember activity calculation). To determine an upper pressure spinel stability limit the following equilibria was used:

$$2\,En + Sp \leftrightarrows Py + Fo \qquad (4)$$

Equilibria (4) involves the following end-members in natural phases: enstatite (En) in othopyroxene, spinel (Sp), pyrope (Py = $Mg_3Al_2Si_3O_{12}$) in garnet and forsterite (Fo) in olivine. A value of unity was assumed for pyrope (with the exception of garnet bearing samples where the calculated activity of garnet was used), and the calculated activity for other mineral endmembers was used. Spinel stability results are given in Table 1 and were used to ensure that the values of pressure used in estimates of fluid fugacities were consistent with the stability of spinel in each sample.

Thermometry results are given in Table 2, shown are the results from the Brey and Köhler, 1990 Ca-in-OPX geothermometer as modified by Nimis and Grütter, 2010 (BKNG), the Taylor, 1998 two pyroxene thermometer (TA98), and the single pyroxene thermometer of Nimis and Taylor, 2000 (NT). Nimis and Grütter, 2010 argue that differences larger than 90° (at TA98 < 900°), 70° (at TA98 900 – 1,200°C), or 50° (at TA98 > 1,200°C) between TA98 and BKNG, which is twice the standard error, represent pyroxene analyses that are likely in disequilibrium with one another. The temperatures estimated for the samples in this study ranged from 650 to 930˚C using the TA98 geo-thermometer. In almost all cases, the differences between the three formulations of the three pyroxene geo-thermometers are significantly less than those outlined by Nimis and

Grütter, 2010 and described above, a result that is consistent with accurate estimates of temperature of mineral equilibration.

For samples Bestiac, PL-4, PTT1, Almklovdalen, and CATRINITY, temperatures were calculated using the compositions of pyroxene rims. This approach is consistent with the textural relations in these samples which indicate that amphibole growth may have occurred late in the samples history with amphibole often replacing pyroxenes (Bestiac, PL-4, and CATRINITY), occurring as small matrix grains likely grown during deformation (PTT1), or occurring in kelyphite texture as well as in the matrix suggesting growth during uplift (Almklovdalen). In these samples, temperatures determined from rim compositions produced the smallest differences between the three pyroxene geothermometers, and as such likely represent equilibration temperatures (see previous paragraph). In samples from New Caledonia cpx occurs as small (<100 μm) accessory grains with no clear chemical zonation and opx grains were clearly chemically zoned. In the New Caledonia samples opx rim compositions were used in conjunction with cpx analysis which produced the smallest variance amongst thermometers (which was not necessarily the rim analysis). Table 2 shows the maximum temperature from the core of opx grains in samples using the BKNG thermometer (labeled BKNG (core)). Most samples exhibit higher temperatures using opx core analyses than rim analyses suggesting these samples likely re-equilibrated during uplift and emplacement at the surface.

Samples PL-4 and Bestiac are spinel bearing peridotites and as such the assumed pressure of 15 kbar was used. For the New Caledonia samples (KA04-17A1, BG02-4B1A, BG02-7A1B, and BG04-13A1A) V. Chatzaras (personal communication) combined geothermometry results with numerical models of the thermal structure of oceanic transform faults (Behn, Boettcher and Hirth, 2007; Roland, Behn and Hirth, 2010) to estimate a pressure of 4 - 7 kbar. Given the lower

pressure stability limits of the spinels (5.6 to 6.4 kbar, Table 1), in New Caledonia samples a pressure of 7 kbar was used for these samples. Al-in-OPX barometry was applied to sample Almklovdalen which results in pressure estimates of 26 kbar when opx rim compositions are used and 30 kbar when opx core compositions are used. Almklovdalen also contains spinel, for which an upper pressure stability limit was calculated using THERMOCALC software (Holland and Powell, 2011) and estimated to be 12.6 kbar, which is significantly lower than the pressure estimated from the Al-in-OPX barometer. Given the upper stability limit of the spinel, kelyphite texture at garnet rims (which potentially represents retrograde reaction of garnet), and compositional zoning present within minerals, it is likely that the smaller matrix minerals equilibrated during depressurization and uplift and were no longer in equilibrium with the garnets, and, therefore, a pressure of 12.6 kbar was used in this sample. Newman *et al.*, 1999 determined pressures of equilibration to range from 5 – 10 kbar for plagioclase bearing samples from Turon de Técouère. Sample PTT1 is from the same locality and likely experienced equilibration conditions similar to those studied in Newman *et al.*, 1999, and as such, a pressure of 8 kbar was used. Equilibria (3) produced a pressure of 5.8 kbar for sample CATRINITY and is the pressure used in subsequent calculations.

For most samples, the results of pressure and temperature determinations in this work are in good agreememnt with P-T determinations from previous studies performed at each respective locality (see Geologic Setting section). Sample Almklovdalen records lower pressure and temperatures than those reported by Kang, Lamb and Drury, 2017 for the WGR. However, similar to the samples in their study, sample Almklovdalen falls close to the P-T uplift path of Spengler *et al.*, 2009, which suggests that this sample equilibrated at shallower conditions, but is still in accordance with the P-T paths of other peridotites in the WGR.

Table 1. Stability limits of Spinel

Sample	Pressure Stability Limit (kb)	
	Lower	Upper
PTT1	3.5	26.4
PL-4	4.5	25.6
Bestiac	4.6	26.8
Almklovdalen	4.4	12.6
CATRINITY	5.1	30.4
KA04-17A1	5.7	25.1
BG02-4B1A	5.6	25.5
BG02-7A1B	5.6	25.1
BG04-13A1A	6.4	24.0

Table 2. Temperature estimates

Sample (pressure)	Temperature			
	BKNG	T98	NT	BKNG (core)
PTT1 (8 kb)	660	**680**	710	820
PL-4 (15 kb)	720	**760**	780	960
Bestiac (15 kb)	770	**830**	840	860
Almklovdalen (12.6 kb)	500	**660**	670	540
CATRINITY (5.8 kb)	900	**900**	940	1190
KA04-17A1 (7 kb)	810	**800**	840	1050
BG02-4B1A (7 kb)	770	**800**	830	1170
BG02-7A1B (7 kb)	800	**800**	820	1220
BG04-13A1A (7 kb)	880	**860**	890	1100

DEHYDRATION EQUILIBRIA

Dehydration reactions may be used to determine a value of aH_2O at a specific pressure and temperature. For examples, dehydration equilibria involving amphibole and biotite have been applied to lower crustal rocks to estimate aH_2O (e.g. Lamb and Valley, 1988). Additionally, this technique has been applied to estimate aH_2O from amphibole bearing mantle peridotites (Lamb and Popp, 2009; Kang, Lamb and Drury, 2017; Hunt and Lamb, 2019). This study will employ similar methods using the following dehydration equilibria:

$$En + 2\,Parg \leftrightarrows 2\,Fo + 4\,Di + 2\,Jd + 2\,Sp + 2\,H_2O \quad (5)$$

$$2\,Tr + 2\,Fo \leftrightarrows 5\,En + 4\,Di + 2\,H_2O \quad (6)$$

Reaction (5) involves end members pargasite (Parg = $NaCa_2Mg_4Al_3Si_6O_{22}(OH)_2$) in amphibole, enstatite (En = $MgSiO_3$) in orthopyroxene, jadeite (Jd = $NaAlSi_2O_6$) and diopside (Di = $CaMgSi_2O_6$) in clinopyroxene, forsterite (Fo = Mg_2SiO_4) in olivine, and spinel (Sp = $MgAl_2O_4$) in spinel. These end-members were chosen by Lamb and Popp (2009) because of their relatively high concentration in phases from upper mantle peridotites which helps minimize uncertainties when determining end-member activities in minerals. The exception to this is the jadeite end-member in clinopyroxene whose concentrations tend to be relatively low in upper mantle rocks. However, this disadvantage is, at least in part, mitigated by the relative abundance of experimental data that is available to constrain a-X relationships of clinopyroxene (Green, Holland and Powell, 2007).

The second reaction (6) involves endmembers tremolite (Tr = $Ca_2Mg_5Si_8O_{22}(OH)_2$) in amphibole, forsterite in olivine, enstatite in orthopyroxene, and diopside in clinopyroxene. This reaction largely avoids phases where the concentration of the end-member in the natural phase is small (such as, in reaction 3, with regard to the jadeite component in cpx). It does, however, involve the tremolite component in amphibole, which may be smaller than the pargasite component in

mantle amphiboles. However, the amphiboles in this study have relatively large tremolite concentrations. Additionally, reaction (6) tends to produce results with lower uncertainty, as compared to reaction (5), as determined by THERMOCALC (Holland and Powell, 2011).

Lamb and Popp (2009) compared several approaches to calculating activities of mineral end-members in natural phases, and explicitly compared differences between using ideal models, THERMOCALC (Holland and Powell, 2011), or MELTS (Sack and Ghiorso, 1989) software packages for those calculations. They demonstrated that model selection had only small effects on the outcome of their aH_2O calculations. Endmember activities in this study are calculated using the models present in the AX62 software, which is consistent with the self-consistent thermodynamic database of Holland and Powell, 2011. A full discussion of the selection process for representative chemical analyses is given below. The resulting activities of mineral endmembers are shown in Table 3.

Table 3. Activities of mineral endmembers

Sample	*a Di*	*a*Jd	*a*En	*a*Fo	*a*Sp	*a*Parg	*a*Tr
PTT1	0.69	0.11	0.75	0.81	0.62	-	0.06
PL-4	0.70	0.12	0.75	0.82	0.69	0.20	0.03
Bestiac	0.66	0.13	0.73	0.81	0.66	0.24	0.04
Almklovdalen	0.81	0.06	0.83	0.85	0.71	0.30	0.24
CATRINITY	0.77	0.01	0.73	0.80	0.50	0.25	0.08
KA04-17A1	0.89	-	0.80	0.85	0.65	0.04	0.59
BG02-4B1A	0.88	-	0.79	0.84	0.63	-	0.63
BG02-7A1B	0.88	-	0.82	0.84	0.61	0.01	0.57
BG04-13A1A	0.87	-	0.84	0.84	0.50	0.11	0.45

(-) indicates samples with parg or jd activity lower than uncertainty

Activities of H_2O were calculated using equilibria (6) and when possible (5) on all samples using dataset 6.2 in THERMOCALC version 3.40 (Holland and Powell, 2011), results are shown in Table 4. To evaluate the uncertainty for values of aH_2O calculations, values of aH_2O were recalculated at: 60 °C (Almklovdalen, KA04-17A1, BG02-4B1A, BG02-7A1B, BG04-13A1A),

90 °C (PTT1 and CATRINITY), and 100 °C (PL-4 and Bestiac), above and below the temperature determined from thermometry. The choice in temperature range for determining uncertainty is derived from the addition of the temperature uncertainty estimated by THERMOCALC and the uncertainty of 30 °C of the TA98 thermometer as reported by Taylor, 1998. Uncertainties in values of aH_2O based on equilibria 6 are listed in Table 4. The lower and upper values for these uncertainties are not equivalent and range from -0.04 to -0.30, and 0.14 to 0.48 respectively.

Table 4. Activities of H_2O

Sample	aH_2O		Uncertainty	
	Rx 6	Rx 5	-	+
PTT1	0.07	-	0.04	0.14
PL-4	0.12	0.08	0.06	0.16
Bestiac	0.27	0.10	0.12	0.31
Almklovdalen	0.21	0.11	0.07	0.18
CATRINITY	0.40	0.78	0.19	0.48
KA04-17A1	0.93	-	0.27	0.34
BG02-4B1A	~1.0	-	0.29	0.29
BG02-7A1B	0.87	-	0.28	0.41
BG04-13A1A	~1.0	-	0.30	0.30

Note: (-) inidicates samples with no parg or no jd component

Using an individual analytical point or an analytical average to calculate activities of olivine species had little (+/- 0.01) effect on resultant activity for all samples. For other mineral species due to chemical zonation present with mineral grains selection of an individual analysis or an analytical average could have relatively large impacts on resultant species activity (+/- 0.20). As discussed above, Nimis and Grütter, 2010 argue that equilibrium between cpx and opx in any given sample can be demonstrated with good agreement between various geothermometers. For samples Bestiac, PL-4, PTT1, CATRINITY and Almklovdalen, agreement between thermometers

was best when using rim compositions for both cpx and opx. As such, we argue that rim compositions of minerals (both porphyroclasts and matrix grains) are most likely to be in equilibrium with one another and are most appropriate to use when performing calculations. As mentioned previously this approach is supported by textural relations present within these samples.

In the samples from New Caledonia clinopyroxene occur as small (<100 μm) accessory grains with variable composition and no clear chemical zonation. In this case, cpx analyses that produced the smallest variance amongst the two-pyroxene geothermometers (which were not necessarily rim compositions) were used. Using an individual point or an analytical average to calculate temperature had a maximum effect of ± 100 on the temperature estimates, whereas these difference in cpx compositions species had little effect on resultant endmember activity of the cpx (maximum of +/- .06).

Amphibole grains in New Caledonia samples were severely fractured and displayed variable chemistry with no clear chemical zonation. Samples KA04-17A1 and BG04-13A1A consistently produce high (near 1.0) aH_2O values from dehydration equilibria regardless of which amphibole analysis is used to calculate amphibole endmember activity. In samples BG02-4B1A and BG02-7A1B aH_2O resulting from dehydration equilibria calculations ranges from .47 - ~1.0 and .37 - 1.0 respectively, depending upon which amphibole analysis is used for endmember activity calculation, with analyses that result in higher tremolite activities also resulting in higher water activities. Tremolitic amphiboles are stable at low temperatures relative to amphiboles that are pargasite-rich (Jenkins, 1983), and tremolite-rich amphiboles are often though to form at lower temperatures than pargasite-rich amphiboles. These samples exhibit evidence of being exposed to a range of temperatures with high temperatures recorded in orthopyroxene cores and lower temperature rims. It is possible that amphibole growth began at higher temperatures producing

pargasitic amphiboles and then, as temperatures decreased during uplift, tremolite rich amphiboles began to grow. Growth of tremolite-rich amphiboles may have continued at temperatures below those recorded by pyroxene thermometry. If so, then, for samples BG02-4B1A and BG02-7A1B, the amphibole compositions that are relatively pargasite-rich may have been stable at the temperatures recorded by the compositions of co-existing pyroxenes and values of aH_2O are approximately 0.5. Alternatively, the pargasite-rich composition may have equilibrated at higher T and the tremolite-rich amphiboles formed at temperatures estimated using two-pyroxene thermometery. In this case values of aH_2O for these two samples (BG02-4B1A and BG02-7A1B) are approximately 1.0. However, because two of the samples (KA04-17A1 and BG04-13A1A) only record high water activities (≈1.0) it is likely that some at least some, if not all, rocks from this sample location experienced relatively H_2O-rich conditions.

OXYGEN FUGACITY

The compositions of coexisting orthopyroxene, olivine, and spinel in mantle peridotites can be used to calculate fO_2 in each sample using a spinel peridotite oxy-barometer that is based on the reaction:

$$6\ Fe_2SiO_4 + O_2 = 3\ Fe_2Si_2O_6 + 2\ Fe_3O_4 \quad (7)$$

Olivine (fa) Orthopyroxene (fs) Spinel (mt)

Where fa is fayalite, fs is ferrosilite, and mt is magnetite. This oxy-barometer was developed and used in several studies (Mattioli and Wood, 1986, 1988; O'Neill and Wall, 1987; Wood, 1990). More recently, Miller, Holland and Gibson, 2016 revised this spinel oxybarometer by using equilibria (7) combined with:

$$3\ Fe_2SiO_4 + 3\ Mg_2SiO_4 + O_2 = 2\ Fe_3O_4 + 3\ MgSiO_3 \quad (8)$$

Olivine (fa) Olivine (fo) Spinel (mt) Orthopyroxene (en)

$$6\ MgAl_2O_4 + 6\ Fe_2SiO_4 + O_2 = 2\ Fe_3O_4 + 3\ MgSiO_3 + 6\ FeAl_2O_4 \quad (9)$$

Spinel (sp) Olivine (fa) Spinel (mt) Orthopyroxene (en) Spinel (hc)

Where fo is fosterite, en is enstatite, sp is spinel, and hc is hercynite. These reactions are solved simultaneously using a least squares method, and utilizing dataset 6.2 of Holland and Powell, 2011's thermodynamic data set. The results of this method are largely driven by the reaction in equation (8). This is potentially advantageous due to the reactions lack of dependence on the ferrosilite endmember which generally has low concentrations in mantle orthopyroxenes and is sensitive to the Fe^{3+} content which is often not measured. Additionally, the reaction involves

the forsterite and enstatite endmembers, which generally have high concentrations in mantle olivines and orthopyroxenes, respectively. Results using the oxybarometers of both Wood, 1990 and Miller, Holland and Gibson, 2016 are shown in Table 5. These values range form from -0.01 to 2.00 $\Delta\log fO_2$ (FMQ), which fall in the range of redox conditions recorded in peridotites from the upper mantle that were analyzed in previous studies (Woodland, Kornprobst and Wood, 1992; Woodland and Koch, 2003).

A program written by T. Holland was used to calculate oxygen fugacities and values of uncertainty. Uncertainties for values of $\log fO_2$ based on the method of Miller, Holland and Gibson, 2016 range from ± 0.30 – 1.68 log bars, with an average uncertainty of ± 0.81.

All values of fO_2 are relatively oxidizing, with most values significantly greater than the fayalite, magnetite, quartz (FMQ) oxygen buffer. These values are also more oxidizing than the upper stability limit of carbon (graphite/diamond) as defined by the reaction of carbon with oxygen to form CO_2 (Graphite - CO_2 buffer). Thus, the values of fO_2 recorded in this study rule out even trace amounts of solid carbon and would not allow for a fluid with a significant amount of CH_4 to co-exist with these rocks (Bryndzia and Wood, 1990; Lamb and Popp, 2009; Kang, Lamb and Drury, 2017).

Table 5. Fugacities of oxygen relative to the FMQ buffer

Sample	$\Delta\log fO_2$ (FMQ)	
	Wood	Miller
PTT1	0.58	0.85
PL-4	0.57	-0.01
Bestiac	0.88	0.64
Almklovdalen	0.47	0.57
CATRINITY	0.80	0.76
KA04-17A1	1.52	1.44
BG02-4B1A	0.98	1.88
BG02-7A1B	1.92	1.75
BG04-13A1A	0.84	0.56

DISCUSSION AND IMPLICATIONS

French Pyrenees

As described previously (see Geologic Setting section) approximately 40 peridotite bodies, typically composed of spinel lherzolite, occur as small isolated bodies in the North Pyrenean metamorphic zone (Fabriès *et al.*, 1989; Fabries *et al.*, 1991). Ti rich pargasite is a common accessory mineral in these peridotite bodies, although it rarely comprises more than 1% of the rock. The presence of these amphiboles has been attributed to a widespread metasomatic event (Fabries *et al.*, 1991). The samples examined in this study from the French Pyrenees, PTT1, PL-4 and Bestiac, all record relatively low water activities (0.12 – 0.27). If a widespread metasomatic event did result in the formation of amphibole it is likely, therefore, that any H_2O that may have been associated with this event was incorporated into the solid phases (e.g. amphibole) and, therefore, these rocks equilibrated at low values of aH_2O.

Although evidence for metasomatism has been identified in a number of orogenic peridotites form the Pyrenees, including the Lherz (Bodinier *et al.*, 1990; Le Roux *et al.*, 2007; Lorand, Alard and Luguet, 2010) and Cassou (Fabriès *et al.*, 1989) bodies, it is not clear that amphibole in all peridotite bodies must have formed via metasomatism. Furthermore, amphiboles that originally formed via metasomatism may have been recrystallized during subsequent deformation. In this case, mineral equilibration might have occurred during deformation. For example, sample PTT1, from the Turon de Técouère orogenic peridotite, is a protomyolonite, and the mineralogy and textures in this samples are similar to protomylonite from this same peridotite body described by Newman *et al.*, 1999. In these rocks porphyroclasts of opx, cpx, sp, and ol occur amongst a fine grain matrix of these same phases, along with amphibole. Newman *et al.*, 1999 interpret the polyphase nature of the matrix to be the result of continuous net transfer

reactions occuring at the margins of porphyoclasts, with grain size reduction occuring via reaction weakening rather than some other deformational mechasim (e.g. dislocation creep). This suggests that matrix grains likely grew during deformation. Amphibole exhibits a range of grain sizes all of which are signficantly smaller than the porphyroclasts in this samples. Although it is possible that some amphbiole existed prior to deformation, most, if not all amphibole in these rocks fromed during deformation, often at the expense of cpx. The presence of this amphibole does not require infiltration of externally-sourced H_2O. Instead the H_2O necessary to grow amphibole during deformation could have been supplied from pre-existing amphiboles, or H_2O contained in NAMs. In either case, deformation occurred at low values of aH_2O (significantly less that one), consistent with the interpretation of Newman *et al.*, 1999.

Several studies have demonstrated that the presence of amphibole in peridotites does not require H_2O rich conditions (Lamb and Valley, 1988; Lamb and Popp, 2009; Hunt and Lamb, 2019). Furthermore, Kang, Lamb and Drury, 2017 demonstrated that amphibole growth may occur in the absence of a lithostatically pressured free fluid phase. The proposed mechanism of amphibole growth facilitated by H_2O present in NAMs may also be responsible for amphibole present in samples PL-4 and Bestiac. Ultimately, this argument could be supported with future analyses of the H-content of NAMs. If the H_2O originated in NAMs that originally had elevated H-contents then the cores of porphyroclasts might preserve these relatively high H-contents.

If our samples did experience mantle metasomatism, then it should be beneficial to measure trace elements present within minerals such as cpx, as trace element systematics can be useful in constraining whether mantle peridotites have experienced interactions with metasomatic agents, and if so, the source and type of metasomatic fluid (Coltorti *et al.*, 2007; Jean *et al.*, 2010; Harvey *et al.*, 2012; le Roex and Class, 2014; Créon *et al.*, 2017; Uenver-Thiele *et al.*, 2017). Preliminary

trace element measurements were made on sample Bestiac where a 200 um thick section was created, and trace elements within cpx were measured via Laser Ablation Inductively Coupled Mass Spectroscopy (details given in Table 6). The workflow of Uenver-Thiele *et al.*, 2017 was adopted for this preliminary attempt at collecting and interpreting the resulting data. The resulting chrondite-normalized REE pattern is shown in Figure 11, in addition to the expected pattern for cpx from group A of Uenver-Thiele *et al.*, 2017. The REE pattern along with La/Ce, Nd/Yb, Zr/Hf ratios, Sr and Ti concentrations, and adherence to melt path predictions (Table 7) classify Bestiac as belonging to group A of Uenver-Thiele *et al.*, 2017. This group is interpreted to have only experienced changes in REE concentrations due to partial melting and to have experienced limited, if any, interaction with a metasomatic fluid (for justification see Uenver-Thiele *et al.*, 2017). The results from this preliminary analysis are not consistent with amphibole growth due to the introduction of a metasomatic fluid and are consistent with small amounts of amphibole in the sample from Bestiac forming from H_2O present within NAMs.

Almklovdalen. Norway

Sample Almklovdalen is from the Western Gneiss region of Norway and, as noted previously, peridotites from this region experienced a prolonged period of uplift as they experienced maximum pressures of approximately 65 kbar (Spengler *et al.*, 2009). The P-T estimate from this sample (≈650˚C at 12.6 kbar) is consistent with estimates of the P-T path followed the rocks of the Western Gneiss region (Spengler *et al.*, 2009) after ultra-high pressure metamorphism. This sample records a value of $aH_2O = 0.21$, similar to H_2O activities estimated from other mantle peridotites from the Western Gneiss Region (Kang, Lamb and Drury, 2017). As noted by Kang, Lamb and Drury, 2017, pressures > 30 kbar are outside the stability field of pargasite (Niida and Green, 1999), and as such, amphibole growth likely occurred during uplift as

a retrograde product after the sample traversed through the stability field of pargasitic amphibole. It might be argued that amphibole growth required the influx of H_2O-bearing fluids. However, at the maximum P-T experienced by these rocks (65 kbar and 920 °), the NAMs present in their samples could have contained enough water to grow the amount of amphibole present within this sample. Consequently, NAMs could have supplied sufficient H to form amphibole and no external source of H_2O would be required (see the discussion in Kang, Lamb and Drury, 2017). In this case amphibole growth consumes much of the available H resulting in equilibration at low values of aH_2O.

California, USA

Sample CATRINITY records a moderate aH_2O value of .40. This sample is derived from the Trinity Ophiolite in California, which as mentioned previously may represent a supra-subduction ophiolite, with some samples in the area displaying evidence for melt/rock interaction (Quick, 1981, 1982; Kelemen, Dick and Quick, 1992; Ceuleneer and Le Sueur, 2008; Jochum *et al.*, 2009; Dygert, Liang and Kelemen, 2016). These melts could potentially be induced from dewatering of a down going slab within the subduction zone, this melt could in-turn transport water into the overlying lithospheric mantle providing the water necessary for amphibole growth. Amphibole in CATRINITY largely occurs near the grain boundaries of pyroxenes, possibly replacing pyroxenes (Figure 5). The association of amphibole with pyroxene grain boundaries may be evidence for infiltration of the above-mentioned melts, as amphibole growth may have occurred in association with fluids/melts migrated around grains as they moved through these peridotite bodies. The moderate water activities recorded in this sample could be the result of water being consumed during amphibole growth, and reinforces the observation that the presence of amphibole does not require high values of aH_2O. As noted earlier trace element systematics can be useful in

constraining whether mantle peridotites have experienced interactions with metasomatic agents such as melts. Future study of the trace elements present in cpx in this sample should lend insight into the extent of melt interaction that this sample may have experienced (e.g. Dygert, Liang and Kelemen, 2016), and in turn, better constrain the mechanism of amphibole growth and generation of moderate aH_2O values.

New Caledonia

Samples KA04-17A1, BG02-4B1A, BG02-7A1B, and BG04-13A1A are challenging with respect to establishing the composition of minerals that equilibrated with one another. This challenge is largely due to amount of serpentine and the variability in the composition of individual minerals and mineral grains, particularly cpx and amphibole. Activities of amphibole endmembers, for example, vary significantly with variations in chemical composition within individual amphibole grains. This suggests a history of amphibole growth, with amphibole compositions changing during the growth of amphibole.

In spite of these complications, and the highly altered nature of these samples, amphibole equilibria suggest equilibration at relatively high water activities (0.87 - ~1.0). These samples from the Bogota Peninsula in New Caledonia, are thought to have been part of a paleo oceanic transform fault. Our values of aH_2O indicate that deformation along this fault likely occurred under water rich conditions.

Infiltration of an H_2O-rich fluid may have occurred throughout much of the history experienced by these samples. Values of aH_2O close to 1.0 are generally consistent the infiltration of H_2O-rich fluids at elevated temperatures (≈800˚C). At lower temperatures continued infiltration of H_2O would explain the widespread serpentinization within these samples.

Implications

Samples KA04-17A1, BG02-4B1A, BG02-7A1B, and BG04-13A1A are, to my knowledge, the first peridotite samples to record relatively high-water activities based on amphibole equilibria. These are the only samples in this suite that are derived from an oceanic transform fault setting. These results are consistent with recent evidence of infiltration of H_2O-rich fluids to relatively great depths based on seismicity studies (e.g. McGuire *et al.*, 2012; Kuna, Nábělek and Braunmiller, 2019) and microstructural and textural analysis of rocks dredged form oceanic transform faults (e.g. Kohli and Warren, 2019).

Samples from other tectonic settings record lower values of aH_2O, typically < 0.5. Amphibole in mantle peridotites are often thought to form by the interaction of peridotites with metasomatic fluids. The samples from the Trinity Ophiolite and the French Pyrenees may contain amphibole that originally formed in this manner (fluid-rock interaction). If so, then amphibole formation likely resulted from a change in the bulk composition of the rock. Components that could be added by a fluid and that are concentrated in amphiboles include Ti, Al, Na, and H_2O. However, values of aH_2O that are < 0.5 indicate that only small amounts of H_2O (if any) were added to the rock. In the extreme case, amphibole could be stabilized by the metasomatic addition of elements such as Ti, Al, and Na and the necessary H could be derived from pre-existing NAMs. This process may account for the formation of amphibole and low values of aH_2O in the samples from the Turon de Técouère and Lherz peridotite bodies in the French Pyrenees. However, metasomatic interaction may not account for amphibole growth in all peridotites from the Pyrenees as evidenced by the preliminary REE measurements made here, which suggest lack of interaction with any metasomatic agent. Additionally, in the case of the sample from Turon de Técouère, mylonite formation occurred during retrograde cooling and uplift and the production of fine-

grained minerals was, at least in part, the result of continuous net-transfer reactions. These reactions may have produced amphibole which could consume H_2O liberated from NAMs during deformation, rather than H_2O introduced via metasomatism.

In other cases, amphibole may form during retrograde uplift and cooling. In the case of peridotites from the WGR of Norway only small amounts of H_2O are required to grow amphibole in the quantities present in these peridotites, and the solubility of H in NAMs at the max P-T conditions of those rocks is such that all H_2O required could have been incorporated within those NAMs.

Most of the amphibole-bearing peridotites in which values of aH_2O have been quantified using mineral equilibria yield values of aH_2O that are significantly less than 1 (Lamb and Popp, 2009; Kang, Lamb and Drury, 2017; Hunt and Lamb, 2019). The results from this work along with these previous reports clearly show that the presence of amphibole does not indicate that mantle samples are "hydrous", or necessarily have high H_2O content, as compared to peridotites that do not contain amphibole.

Ultimately these samples (especially those with high aH_2O) will serve as valuable subjects in future studies that employ methods for measuring NAM H-content within these samples. Experimentally determined diffusion rates of H within NAMs suggests that these minerals are potentially subject to rapid loss of H (Ingrin and Skogby, 2000), and as such, interpreting data from these measurements as being representative of mantle conditions can be difficult. Measuring the H-content of these NAMs will allow for insights into amount of H-loss experienced by NAMs during emplacement and the veracity of using such methods for estimating mantle water content. Further, there is potential for greater insights into the impacts of variables such as mineral chemistry, and oxygen fugacity on retention of H in NAMs. Additionally, the study of REE

concentrations in minerals such as clinopyroxene in these samples should prove useful in constraining the degree of metasomatic interaction in these samples, (e.g. Coltorti *et al.*, 2007; Jean *et al.*, 2010; Harvey *et al.*, 2012; le Roex and Class, 2014; Créon *et al.*, 2017; Uenver-Thiele *et al.*, 2017), and allow for further insights into the role of metasomatism as it related to amphibole formation in peridotites.

Table 6. LA-ICP-MS Data Collection Details

Laser Ablation System	
Make, Model & Type	ESI/New Wave Research, 193 nm excimer
Ablation Cell & Volume	NWR TV2 cell
Laser Wavelength (nm)	193
Pulse Width (ns)	4
Fluence (J cm^{-2})	5.5
Repetition Rate (Hz)	15
Spot Size (µm)	30
Sampling Mode / Pattern	stationary circle
Carrier Gas	He 0.6 l/min, Ar make-up gas 0.8 l/min combined 1/4 of way along sample line
Ablation Duration (secs)	30
Cell Carrier Gas Flow (l/min)	0.6
ICP-MS Instrument	
Make, Model & Type	ThermoScientific iCAP RQ
Sample Introduction	Ablation aerosol directly to injector
RF Power (W)	1550
Make-Up Gas Flow (l/min)	0.8 Ar
Detection System	pulse / analog SEM (analog trigger >2.5M cps)
Masses Measured	29Si, 30Si, 43Ca, 44Ca, 45Sc, 49Ti, 51V, 59Co, 60Ni, 62Ni, 85Rb, 88Sr, 89Y, 90Zr, 93Nb, 137Ba, 139La, 140Ce, 141Pr, 146Nd, 149Sm, 151Eu, 157Gd, 159Tb, 163Dy, 165Ho, 167Er, 169Tm, 173Yb, 175Lu, 177Hf, 181Ta, 208Pb, 232Th, 238U
Integration Time per Peak (sec)	varies, 0.01 to 0.05
Sensitvity / Efficiency (%, element)	7.5 x 10^3 to 10 x 10^3 CPS/ppm (NIST 612)
IC Dead Time (ns)	20
Data Processing	
Gas Blank	10 second on-peak zero subtracted
Calibration Strategy	NIST 612 primary standard, NIST 610 and BCR-2G secondary, Ca internal standard from EPMA analysis
Reference Material Info	NIST 612 and 610 (Jochum *et al.*, 2011) BCR-2G (Jochum *et al.*, 2009)
Data Processing Package Used	Qtegra and Iolite
Quality Control / Validation	Wtd Avgs of primary and secondary standards for each analytical session given in Final Data Table

Table 7. Classification scheme from Uenver-Thiele et al., 2017

Group:	A	B	C	D	Bestiac
La/Ce	0.15 - 0.6	0.4 - 1.4	0.2 - 0.7	0.6 - 2.0	0.25
Nd/Yb	2 - 3.5	2.0 - 11	5 - 35	< 1.5	1.78
Sr(ppm)	60 ± 30	620	620	low	60
Ti (ppm)	> 2800	< 3000	< 3000	low	3467
Zr/Hf	25 - 40	25 - 40	25 - 40	< 20	32
Melt Path	On	On but scattered	Off	Off	On

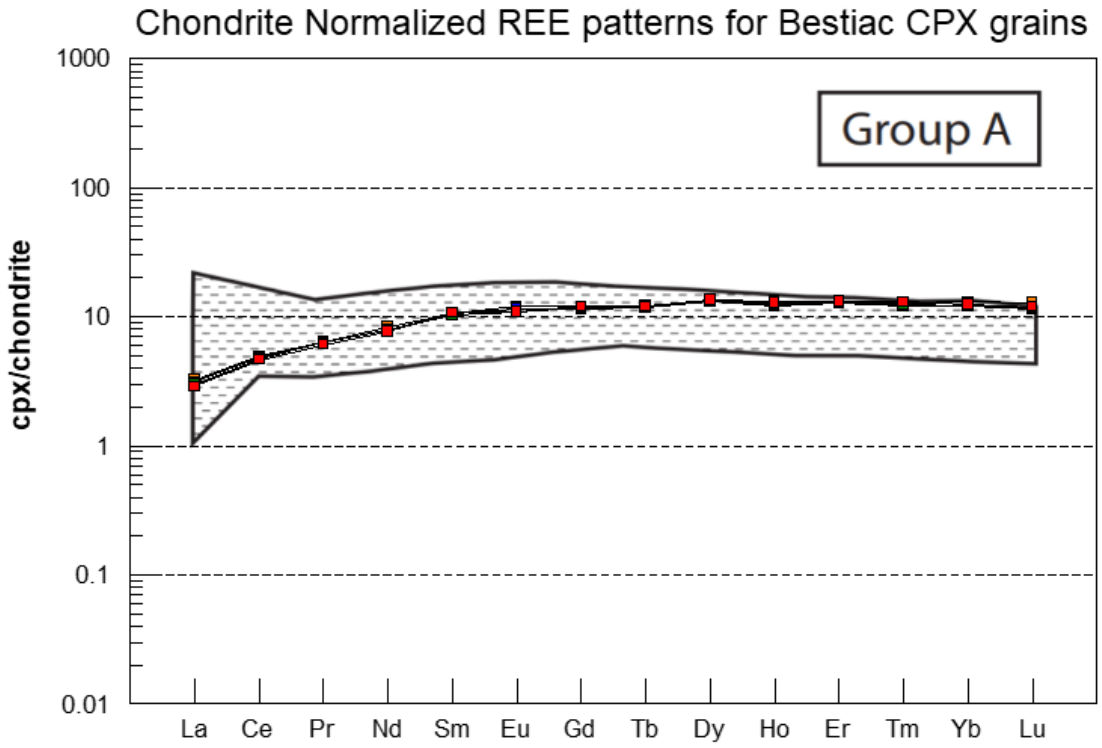

Figure 11. Chondrite-normalized REE patterns for clinopyroxenes modified from Uenver-Thiele *et al.*, 2017. The four different colored squares (orange, blue, red, and green) represent four different grain analyses (average concentration is plotted). Area shaded with dashed lines represents expected group A REE pattern from Uenver-Thiele *et al.*, 2017.

SUMMARY

Dehydration equilibria in this study yields both low aH_2O values (< 0.4) which is similar to other reports of aH_2O in mantle derived peridotites, and high aH_2O values (0.87 – 1.0) which are atypical. Amphibole growth is often attributed to rock/fluid interaction which may be the case in some of these rocks. However, we propose an additional mechanism where NAMs may serve as a reservoir of the H needed to grow amphibole in these rocks. Samples that yield high aH_2O values are all from New Caledonia and interpreted to represent a paleo oceanic transform fault. These high values of aH_2O are consistent with the notion that fluids may circulate through oceanic transform faults to great depths.

REFERENCES

Agrinier, P. *et al.* (1993) 'Metasomatic hydrous fluids in amphibole peridotites from Zabargad Island (Red Sea)', *Earth and Planetary Science Letters*, 120(3–4), pp. 187–205. doi: 10.1016/0012-821X(93)90239-6.

Behn, M. D., Boettcher, M. S. and Hirth, G. (2007) 'Thermal structure of oceanic transform faults', *Geology*. GeoScienceWorld, 35(4), p. 307. doi: 10.1130/G23112A.1.

Bell, D. R. and Rossman, G. R. (1992) 'Water in Earth's mantle: The role of nominally anhydrous minerals', *Science*, pp. 1391–1397. doi: 10.1126/science.255.5050.1391.

Beran, A. and Libowitzky, E. (2006) 'Water in Natural Mantle Minerals II: Olivine, Garnet and Accessory Minerals', *Reviews in Mineralogy and Geochemistry*. GeoScienceWorld, 62(1), pp. 169–191. doi: 10.2138/rmg.2006.62.8.

Beyer, E. E., Griffin, W. L. and O'Reilly, S. Y. (2006) 'Transformation of archaean lithospheric mantle by refertilization: Evidence from exposed peridotites in the Western Gneiss Region, Norway', *Journal of Petrology*. doi: 10.1093/petrology/egl022.

Bodinier, J. L. *et al.* (1990) 'Mechanisms of mantle metasomatism: Geochemical evidence from the lherz orogenic peridotite', *Journal of Petrology*. doi: 10.1093/petrology/31.3.597.

Bodinier, J. L., Dupuy, C. and Dostal, J. (1988) 'Geochemistry and petrogenesis of Eastern Pyrenean peridotites', *Geochimica et Cosmochimica Acta*. Pergamon, 52(12), pp. 2893–2907. doi: 10.1016/0016-7037(88)90156-1.

Brey, G. P. and Köhler, T. (1990) 'Geothermobarometry in four-phase lherzolites II. new thermobarometers, and practical assessment of existing thermobarometers', *Journal of Petrology*, 31(6), pp. 1353–1378. doi: 10.1093/petrology/31.6.1353.

Brueckner, H. K. and Medaris, L. G. (1998) 'A tale of two orogens: the contrating T-P-t history

and geochemical evolution of mantle in high- and ultrahigh-pressure metamorphic terranes of the Norwegian Caledonides and the Czech Variscides', *Schweizerische Mineralogische und Petrographische Mitteilungen*.

Bryndzia, L. T. and Wood, B. J. (1990) 'Oxygen thermobarometry of abyssal spinel peridotites: the redox state and C-O-H volatile composition of the Earth's sub-oceanic upper mantle', *American Journal of Science*. doi: 10.2475/ajs.290.10.1093.

Burnham, C. W. (1979) 'The importance of volatile constituents', in Yoder, H. S. (ed.) *The Evolution of Igenous Rocks* . Princeton: Princeton University Press, pp. 439–482.

Carswell, T. and van Roermund, H. L. M. (2003) 'The occurrence and interpretation of garnet peridotite bodies in the Western Gneiss Region of Norway', in Carswell, D. A. (ed.) *Guidebook to the Post-Selje Eclogite Field Symposium Field Excursion*. Trondheim: Norges Geologiske Undersøkelse.

Ceuleneer, G. and Le Sueur, E. (2008) 'The Trinity ophiolite (California): the strange association of fertile mantle peridotite with ultra-depleted crustal cumulates', *Bulletin de la Societe Geologique de France*. GeoScienceWorld, 179(5), pp. 503–518. doi: 10.2113/gssgfbull.179.5.503.

Chen, J. *et al.* (2002) 'Effect of water on olivine-wadsleyite phase boundary in the $(Mg, Fe)_2SiO_4$ system', *Geophysical Research Letters*. John Wiley & Sons, Ltd, 29(18), pp. 22-1-22–4. doi: 10.1029/2001GL014429.

Choukroune, P. *et al.* (1973) 'Bay of Biscay and Pyrenees', *Earth and Planetary Science Letters*. Elsevier, 18(1), pp. 109–118. doi: 10.1016/0012-821X(73)90041-1.

Clerc, C. *et al.* (2012) 'Exhumation of subcontinental mantle rocks: evidence from ultramafic-bearing clastic deposits nearby the Lherz peridotite body, French Pyrenees', *Bulletin de la*

Societe Geologique de France. GeoScienceWorld, 183(5), pp. 443–459. doi: 10.2113/gssgfbull.183.5.443.

Clerc, C. *et al.* (2015) 'High-temperature metamorphism during extreme thinning of the continental crust: A reappraisal of the North Pyrenean passive paleomargin', *Solid Earth*. doi: 10.5194/se-6-643-2015.

Cluzel, D. *et al.* (2006) 'Earliest Eocene (53 Ma) convergence in the Southwest Pacific: evidence from pre-obduction dikes in the ophiolite of New Caledonia', *Terra Nova*. John Wiley & Sons, Ltd (10.1111), 18(6), pp. 395–402. doi: 10.1111/j.1365-3121.2006.00704.x.

Cluzel, D., Aitchison, J. C. and Picard, C. (2001) 'Tectonic accretion and underplating mafic terranes in the late Eocene intraoceanic fore-arc of New Caledonia (Southwest Pacific): Geodynamic implications', *Tectonophysics*. doi: 10.1016/S0040-1951(01)00148-2.

Collot, J. Y. *et al.* (1987) 'Overthrust emplacement of New Caledonia Ophiolite: Geophysical evidence', *Tectonics*. doi: 10.1029/TC006i003p00215.

Coltorti, M. *et al.* (1999) 'Carbonatite Metasomatism of the Oceanic Upper Mantle: Evidence from Clinopyroxenes and Glasses in Ultramafic Xenoliths of Grande Comore, Indian Ocean', *Journal of Petrology*. Oxford University Press, 40(1), pp. 133–165. doi: 10.1093/petroj/40.1.133.

Coltorti, M. *et al.* (2004) 'Amphibole genesis via metasomatic reaction with clinopyroxene in mantle xenoliths from Victoria Land, Antarctica', *Lithos*. Elsevier, 75(1–2), pp. 115–139. doi: 10.1016/J.LITHOS.2003.12.021.

Coltorti, M. *et al.* (2007) 'Amphiboles from suprasubduction and intraplate lithospheric mantle', *Lithos*, 99(1–2), pp. 68–84. doi: 10.1016/j.lithos.2007.05.009.

Conquéré, F. and Fabriès, J. (1984) 'Chemical Disequilibrium and Its Thermal Significance in Spinel-Peridotites from the Lherz and Freychinede Ultramafic Bodies (Ariege; French

Pyrenees)', *Developments in Petrology*. Elsevier, 11(2), pp. 319–331. doi: 10.1016/B978-0-444-42274-3.50033-0.

Crawford, A. J., Meffre, S. and Symonds, P. A. (2003) '120 to 0 Ma tectonic evolution of the southwest Pacific and analogous geological evolution of the 600 to 220 Ma Tasman Fold Belt System', in *Special Paper of the Geological Society of America*. doi: 10.1130/0-8137-2372-8.383.

Créon, L. *et al.* (2017) 'Slab-derived metasomatism in the Carpathian-Pannonian mantle revealed by investigations of mantle xenoliths from the Bakony-Balaton Highland Volcanic Field', *Lithos*, 286–287, pp. 534–552. doi: 10.1016/j.lithos.2017.06.004.

Crowley, J. W., Gerault, M. and O'Connell, R. J. (2011) 'On the relative influence of heat and water transport on planetary dynamics', *Earth and Planetary Science Letters*, 310(3–4), pp. 380–388. doi: 10.1016/j.epsl.2011.08.035.

Dawson, J. B. (1980) *Kimberlites and Their Xenoliths*. Berlin, Heidelberg: Springer Berlin Heidelberg (Minerals and Rocks). doi: 10.1007/978-3-642-67742-7.

Demouchy, S. *et al.* (2015) 'Characterization of hydration in the mantle lithosphere: Peridotite xenoliths from the Ontong Java Plateau as an example', *Lithos*, 212–215, pp. 189–201. doi: 10.1016/j.lithos.2014.11.005.

Demouchy, S. and Bolfan-Casanova, N. (2016) 'Distribution and transport of hydrogen in the lithospheric mantle: A review', *Lithos*, pp. 402–425. doi: 10.1016/j.lithos.2015.11.012.

Dubois, J., Launay, J. and Recy, J. (1974) 'Uplift movements in New Caledonia-Loyalty Islands area and their plate tectonics interpretation', *Tectonophysics*. doi: 10.1016/0040-1951(74)90134-6.

Dygert, N., Liang, Y. and Kelemen, P. B. (2016) 'Formation of Plagioclase Lherzolite and

Associated Dunite–Harzburgite–Lherzolite Sequences by Multiple Episodes of Melt Percolation and Melt–Rock Reaction: an Example from the Trinity Ophiolite, California, USA', *Journal of Petrology*. Narnia, 57(4), pp. 815–838. doi: 10.1093/petrology/egw018.

Eissen, J. P. *et al.* (1998) 'Geochemistry and tectonic significance of basalts in the Poya Terrane, New Caledonia', *Tectonophysics*. doi: 10.1016/S0040-1951(97)00183-2.

Fabries, J. *et al.* (1991) 'Evolution of the Upper Mantle beneath the Pyrenees: Evidence from Orogenic Spinel Lherzolite Massifs', *Journal of Petrology*. Narnia, Special_Volume(2), pp. 55–76. doi: 10.1093/petrology/Special_Volume.2.55.

Fabriès, J. *et al.* (1989) 'Evidence for modal metasomatism in the orogenic spinel lherzolite body from caussou (Northeastern Pyrenees, France)', *Journal of Petrology*. doi: 10.1093/petrology/30.1.199.

Fabriès, J. and Conquéré, F. (1983) 'Les lherzolites à spinelle et les pyroxénites à grenat associées de Bestiac (Ariège, France)', *Bulletin de Minéralogie*. Persée - Portail des revues scientifiques en SHS, 106(6), pp. 781–803. doi: 10.3406/bulmi.1983.7700.

Fuis, G. S. *et al.* (1987) 'A geologic interpretation of seismic-refraction results in northeastern California', *Geological Society of America Bulletin*. GeoScienceWorld, 98(1), p. 53. doi: 10.1130/0016-7606(1987)98<53:AGIOSR>2.0.CO;2.

Gaetani, G. A. *et al.* (2014) 'Hydration of mantle olivine under variable water and oxygen fugacity conditions', *Contributions to Mineralogy and Petrology*, 167(2), pp. 1–14. doi: 10.1007/s00410-014-0965-y.

Gaetani, G. A. and Grove, T. L. (1998) 'The influence of water on melting of mantle peridotite', *Contributions to Mineralogy and Petrology*, 131(4), pp. 323–346. doi: 10.1007/s004100050396.

Gasparik, T. (2000) 'An Internally Consistent Thermodynamic Model for the System CaO-MgO-

Al2O3-SiO2 Derived Primarily from Phase Equilibrium Data', *The Journal of Geology*, 108, pp. 103–119. doi: doi:10.1086/314389.

Gee, D. G. *et al.* (2008) 'From the early Paleozoic platforms of Baltica and Laurentia to the Caledonide Orogen of Scandinavia and Greenland', in *Episodes*.

Green, D. H. and Falloon, T. J. (1998) *Pyrolite: A Ringwood Concept and Its Current Expression, The Earth's Mantle: Composition, Structure and Evolution*. doi: 10.1017/CBO9780511573101.010.

Green, D. H. and Falloon, T. J. (2005) 'Primary magmas at mid-ocean ridges, "hotspots," and other intraplate settings: Constraints on mantle potential temperature', *Geological Society of America Special Papers*, 388, pp. 217–247. doi: 10.1130/0-8137-2388-4.217.

Green, E., Holland, T. and Powell, R. (2007) 'An order-disorder model for omphacitic pyroxenes in the system jadeite-diopside-hedenbergite-acmite, with applications to eclogitic rocks', *American Mineralogist*, 92(7), pp. 1181–1189. doi: 10.2138/am.2007.2401.

Harvey, J. *et al.* (2012) 'Deciphering the trace element characteristics in kilbourne hole peridotite xenoliths: Melt-rock interaction and metasomatism beneath the Rio Grande Rift, SW USA', *Journal of Petrology*, 53(8), pp. 1709–1742. doi: 10.1093/petrology/egs030.

Hirth, G. and Kohlstedt, D. L. (1996) 'Water in the oceanic upper mantle: Implications for rheology, melt extraction and the evolution of the lithosphere', *Earth and Planetary Science Letters*, 144(1–2), pp. 93–108. doi: Doi 10.1016/0012-821x(96)00154-9.

Holland, T. J. B. and Powell, R. (2011) 'An improved and extended internally consistent thermodynamic dataset for phases of petrological interest, involving a new equation of state for solids', *Journal of Metamorphic Geology*, 29(3), pp. 333–383. doi: 10.1111/j.1525-1314.2010.00923.x.

Honing, D. and Spohn, T. (2016) ‘Continental growth and mantle hydration as intertwined feedback cycles in the thermal evolution of Earth’, *Physics of the Earth and Planetary Interiors*, 255, pp. 27–49. doi: 10.1016/j.pepi.2016.03.010.

Hunt, L. E. and Lamb, W. M. (2019) ‘Application of mineral equilibria to estimate fugacities of H2O, H2, and O2 in mantle xenoliths from the southwestern U.S.A.’, *American Mineralogist*. GeoScienceWorld, 104(3), pp. 333–347. doi: 10.2138/am-2019-6602.

Ingrin, J. and Skogby, H. (2000) ‘Hydrogen in nominally anhydrous upper-mantle minerals: concentration levels and implications’, *European Journal of Mineralogy*, 12(3), pp. 543–570. doi: 10.1127/0935-1221/2000/0012-0543.

Jean, M. M. *et al.* (2010) ‘Melt extraction and melt refertilization in mantle peridotite of the Coast Range ophiolite: An LA-ICP-MS study’, *Contributions to Mineralogy and Petrology*, 159(1), pp. 113–136. doi: 10.1007/s00410-009-0419-0.

Jenkins, D. M. (1983) ‘Stability and composition relations of calcic amphiboles in ultramafic rocks’, *Contributions to Mineralogy and Petrology*. doi: 10.1007/BF00371206.

Jenkins, D. M. and Newton, R. C. (1979) ‘Experimental determination of the spinel peridotite to garnet peridotite inversion at 900° C and 1,000° C in the system CaO-MgO-Al2O3-SiO2, and at 900° C with natural garnet and olivine’, *Contributions to Mineralogy and Petrology*, 68(4), pp. 407–419. doi: 10.1007/BF01164525.

Jochum, K. P. *et al.* (2009) ‘Geostandards and Geoanalytical Research Bibliographic Review 2008’, *Geostandards and Geoanalytical Research*. John Wiley & Sons, Ltd (10.1111), 33(4), pp. 501–505. doi: 10.1111/j.1751-908X.2009.00083.x.

Jochum, K. P. *et al.* (2011) ‘Determination of Reference Values for NIST SRM 610-617 Glasses Following ISO Guidelines’, *Geostandards and Geoanalytical Research*. John Wiley & Sons, Ltd

(10.1111), 35(4), pp. 397–429. doi: 10.1111/j.1751-908X.2011.00120.x.

Kang, P., Lamb, W. M. and Drury, M. (2017) 'Using mineral equilibria to estimate H2O activities in peridotites from the Western Gneiss Region of Norway', *American Mineralogist*, 102(5), pp. 1021–1036. doi: 10.2138/am-2017-5915.

Karato, S. I. (1985) 'Defects and plastic deformation in olivine', in S.I. Karato, M. T. (ed.) *Rheology of Solids and the Earth* . U.K.: Oxford University Press, pp. 176–208.

Karato, S. and Jung, H. (1998) 'Water, partial melting and the origin of the seismic low velocity and high attenuation zone in the upper mantle', *Earth and Planetary Science Letters*, 157(3–4), pp. 193–207. doi: Doi 10.1016/S0012-821x(98)00034-X.

Kelemen, P. B., Dick, H. J. B. and Quick, J. E. (1992) 'Formation of harzburgite by pervasive melt/rock reaction in the upper mantle', *Nature*. Nature Publishing Group, 358(6388), pp. 635–641. doi: 10.1038/358635a0.

King, P. L. *et al.* (1999) 'Oxy-substitution and dehydrogenation in mantle-derived amphibole megacrysts', *Geochimica et Cosmochimica Acta*, 63(21), pp. 3635–3651. doi: 10.1016/S0016-7037(99)00162-3.

Klemme, S. and O'Neill, H. S. C. (2000) 'The near-solidus transition from garnet lherzolite to spinel lherzolite', *Contributions to Mineralogy and Petrology*, 138(3), pp. 237–248. doi: 10.1007/s004100050560.

Köhler, T. P. and Brey, G. P. (1990) 'Calcium exchange between olivine and clinopyroxene calibrated as a geothermobarometer for natural peridotites from 2 to 60 kb with applications', *Geochimica et Cosmochimica Acta*. doi: 10.1016/0016-7037(90)90226-B.

Kohli, A. H. and Warren, J. M. (2019) 'Evidence for a deep hydrologic cycle on oceanic transform faults', *Journal of Geophysical Research: Solid Earth*. John Wiley & Sons, Ltd, p.

2019JB017751. doi: 10.1029/2019JB017751.

Korenaga, J. (2011) ‘Thermal evolution with a hydrating mantle and the initiation of plate tectonics in the early Earth’, *Journal of Geophysical Research-Solid Earth*, 116. doi: Artn B1240310.1029/2011jb008410.

Kostenko, O. *et al.* (2002) ‘The mechanism of fluid infiltration in peridotites at Almklovdalen, western Norway’, *Geofluids*. doi: 10.1046/j.1468-8123.2002.00038.x.

Krogh, E. J. (1977) ‘Evidence of Precambrian continent–continent collision in Western Norway’, *Nature*. Nature Publishing Group, 267(5606), pp. 17–19. doi: 10.1038/267017a0.

Kuna, V. M., Nábělek, J. L. and Braunmiller, J. (2019) ‘Mode of slip and crust–mantle interaction at oceanic transform faults’, *Nature Geoscience*. Nature Publishing Group, 12(2), pp. 138–142. doi: 10.1038/s41561-018-0287-1.

Kushiro, I., Yoder, H. S. and Mysen, B. O. (1976) ‘Viscosities of Basalt and Andesite Melts at High-Pressures’, *Journal of Geophysical Research*, 81(35), pp. 6351–6356. doi: DOI 10.1029/JB081i035p06351.

LaFehr, T. R. (1966) ‘Gravity in the Eastern Klamath Mountains, California’, *GSA Bulletin*. GeoScienceWorld, 77(11), pp. 1177–1190. doi: 10.1130/0016-7606(1966)77[1177:gitekm]2.0.co;2.

Lagabrielle, Y. and Bodinier, J. L. (2008) ‘Submarine reworking of exhumed subcontinental mantle rocks: Field evidence from the Lherz peridotites, French Pyrenees’, *Terra Nova*. doi: 10.1111/j.1365-3121.2007.00781.x.

Lagabrielle, Y., Labaume, P. and de Saint Blanquat, M. (2010) ‘Mantle exhumation, crustal denudation, and gravity tectonics during Cretaceous rifting in the Pyrenean realm (SW Europe): Insights from the geological setting of the lherzolite bodies’, *Tectonics*. doi:

10.1029/2009TC002588.

Lamb, W. M. *et al.* (2012) 'Determination of Fe3+/Fe using the electron microprobe: A calibration for amphiboles', *American Mineralogist*, 97(5–6), pp. 951–961. doi: 10.2138/am.2012.3963.

Lamb, W. M. and Popp, R. K. (2009) 'Amphibole equilibria in mantle rocks: Determining values of mantle a(H2O) and implications for mantle H2O contents', *American Mineralogist*, 94(1), pp. 41–52. doi: 10.2138/am.2009.2950.

Lamb, W. M. and Valley, J. W. (1988) 'Granulite facies amphibole and biotite equilibria, and calculated peak-metamorphic water activities', *Contributions to Mineralogy and Petrology*, 100(3), pp. 349–360. doi: 10.1007/BF00379744.

Lipman, P. W. (1964) 'Structure and origin of an ultramafic pluton in the Klamath Mountains, California', *American Journal of Science*. American Journal of Science, 262(2), pp. 199–222. doi: 10.2475/ajs.262.2.199.

Liu, C.-Z. *et al.* (2010) 'Anorthitic plagioclase and pargasitic amphibole in mantle peridotites from the Yungbwa ophiolite (southwestern Tibetan Plateau) formed by hydrous melt metasomatism', *Lithos*. Elsevier, 114(3–4), pp. 413–422. doi: 10.1016/J.LITHOS.2009.10.008.

Lorand, J. P., Alard, O. and Luguet, A. (2010) 'Platinum-group element micronuggets and refertilization process in Lherz orogenic peridotite (northeastern Pyrenees, France)', *Earth and Planetary Science Letters*. doi: 10.1016/j.epsl.2009.11.017.

MacGregor, I. D. (2015) 'Empirical geothermometers and geothermobarometers for spinel peridotite phase assemblages', *International Geology Review*. Taylor & Francis, 57(15), pp. 1940–1974. doi: 10.1080/00206814.2015.1045307.

Mattioli, G. S. and Wood, B. J. (1986) 'Upper mantle oxygen fugacity recorded by spinel

lherzolites', *Nature*. Nature Publishing Group, 322(6080), pp. 626–628. doi: 10.1038/322626a0.

Mattioli, G. S. and Wood, B. J. (1988) 'Magnetite activities across the MgAl2O4-Fe3O4 spinel join, with application to thermobarometric estimates of upper mantle oxygen fugacity', *Contributions to Mineralogy and Petrology*, 98(2), pp. 148–162. doi: 10.1007/BF00402108.

McGuire, J. J. *et al.* (2012) 'Variations in earthquake rupture properties along the Gofar transform fault, East Pacific Rise', *Nature Geoscience*, 5(5), pp. 336–341. doi: 10.1038/ngeo1454.

Medaris, L. G. (1984) 'A geothermobarometric investigation of garnet peridotites in the Western Gneiss Region of Norway', *Contributions to Mineralogy and Petrology*. Springer-Verlag, 87(1), pp. 72–86. doi: 10.1007/BF00371404.

Miller, W. G. R., Holland, T. J. B. and Gibson, S. A. (2016) 'Garnet and spinel oxybarometers: New internally consistent multi-equilibria models with applications to the oxidation state of the lithospheric mantle', *Journal of Petrology*, 57(6), pp. 1199–1222. doi: 10.1093/petrology/egw037.

Mori, T. (1977) *Geothermometry of Spinel Lherzolites, Contrib. Mineral. Petrol*. Available at: https://link.springer.com/content/pdf/10.1007%2FBF00374556.pdf (Accessed: 15 January 2019).

Mosenfelder, J. L. *et al.* (2006) 'Hydrogen incorporation in natural mantle olivines', in *Geophysical Monograph Series*, pp. 45–56. doi: 10.1029/168GM05.

Nakagawa, T., Nakakuki, T. and Iwamori, H. (2015) 'Water circulation and global mantle dynamics: Insight from numerical modeling', *Geochemistry, Geophysics, Geosystems*. John Wiley & Sons, Ltd, 16(5), pp. 1449–1464. doi: 10.1002/2014GC005701.

Newman, J. *et al.* (1999) 'Deformation processes in a peridotite shear zone: reaction-softening by an H2O-deficient, continuous net transfer reaction', *Tectonophysics*. Elsevier, 303(1–4), pp.

193–222. doi: 10.1016/S0040-1951(98)00259-5.

Nickel, K. G. and Green, D. H. (1985) ‘Empirical geothermobarometry for garnet peridotites and implications for the nature of the lithosphere, kimberlites and diamonds’, *Earth and Planetary Science Letters,* 73(1), pp. 158–170. doi: 10.1016/0012-821X(85)90043-3.

Nicolas, A. (1989) ‘Structures of ophiolites and dynamics of oceanic lithosphere’, *Structures of ophiolites and dynamics of oceanic lithosphere*.

Niida, K. and Green, D. H. (1999) ‘Stability and chemical composition of pargasitic amphibole in MORB pyrolite under upper mantle conditions’, *Contributions to Mineralogy and Petrology*. Springer Berlin Heidelberg, 135(1), pp. 18–40. doi: 10.1007/s004100050495.

Nimis, P. and Grütter, H. (2010) ‘Internally consistent geothermometers for garnet peridotites and pyroxenites’, *Contributions to Mineralogy and Petrology*, 159(3), pp. 411–427. doi: 10.1007/s00410-009-0455-9.

Nimis, P. and Taylor, W. R. (2000) ‘Single clinopyroxene thermobarometry for garnet peridotites. Part I. Calibration and testing of a Cr-in-Cpx barometer and an enstatite-in-Cpx thermometer’, *Contributions to Mineralogy and Petrology*, 139(5), pp. 541–554. doi: 10.1007/s004100000156.

Nimis, P. and Trommsdorff, V. (2001) ‘Revised Thermobarometry of Alpe Arami and other Garnet Peridotites from the Central Alps’, *Journal of Petrology*, 42(1), pp. 103–115. doi: 10.1093/petrology/42.1.103.

Nkouandou, O. F. and Temdjim, R. (2011) ‘Petrology of spinel lherzolite xenoliths and host basaltic lava from Ngao Voglar volcano, Adamawa Massif (Cameroon Volcanic Line, West Africa): equilibrium conditions and mantle characteristics’, *Journal of Geosciences*, 56, pp. 375–387. doi: 10.3190/jgeosci.108.

O'Neill, H. S. C. and Wall, V. J. (1987) 'The olivine - orthopyroxene - spinel oxygen geobarometer, the nickel precipitation curve, and the oxygen fugacity of the earth's upper mantle', *Journal of Petrology*, 28(6), pp. 1169–1191. doi: 10.1093/petrology/28.6.1169.

O'Neill, H. S. C. and Wood, B. J. (1979) 'An experimental study of Fe-Mg partitioning between garnet and olivine and its calibration as a geothermometer', *Contributions to Mineralogy and Petrology*, 70(1), pp. 59–70. doi: 10.1007/BF00371872.

Peslier, A. H. *et al.* (2010) 'Olivine water contents in the continental lithosphere and the longevity of cratons', *Nature*, 467(7311), pp. 78–81. doi: 10.1038/nature09317.

Peslier, A. H. *et al.* (2017) 'Water in the Earth's Interior: Distribution and Origin', *Space Science Reviews*. Springer Netherlands, 212(1–2), pp. 743–810. doi: 10.1007/s11214-017-0387-z.

Pirard, C., Hermann, J. and O'neill, H. S. C. (2013) 'Petrology and geochemistry of the crust-mantle boundary in a Nascent Arc, Massif du Sud Ophiolite, New Caledonia, SW Pacific', *Journal of Petrology*. doi: 10.1093/petrology/egt030.

Popp, R. K. *et al.* (1995) 'An experimental study of phase equilibria and Fe oxy-component in kaersutitic amphibole: implications for the fH2and aH2O in the upper mantle', *American Mineralogist*. GeoScienceWorld, 80(5–6), pp. 534–548. doi: 10.2138/am-1995-5-613.

Prinzhofer, A. and Nicolas, A. (1980) 'The Bogota Peninsula, New Caledonia: A Possible Oceanic Transform Fault', *The Journal of Geology*. doi: 10.1086/628523.

Quick, J. E. (1981) 'Petrology and petrogenesis of the Trinity peridotite, An upper mantle diapir in the eastern Klamath Mountains, northern California', *Journal of Geophysical Research*. John Wiley & Sons, Ltd, 86(B12), p. 11837. doi: 10.1029/JB086iB12p11837.

Quick, J. E. (1982) 'The origin and significance of large, tabular dunite bodies in the Trinity peridotite, northern California', *Contributions to Mineralogy and Petrology*. Springer-Verlag,

78(4), pp. 413–422. doi: 10.1007/BF00375203.

Ranalli, G. (1995) *Rheology of the Earth*. London: Chapman and Hall.

van Roermund, H. L. M. and Drury, M. R. (1998) 'Ultra-high pressure (P > 6 GPa) garnet peridotites in Western Norway: exhumation of mantle rocks from > 185 km depth', *Terra Nova*, 10, pp. 295–301.

le Roex, A. and Class, C. (2014) 'Metasomatism of the Pan-African lithospheric mantle beneath the Damara Belt, Namibia, by the Tristan mantle plume: Geochemical evidence from mantle xenoliths', *Contributions to Mineralogy and Petrology*, 168(2), pp. 1–21. doi: 10.1007/s00410-014-1046-y.

Roland, E., Behn, M. D. and Hirth, G. (2010) 'Thermal-mechanical behavior of oceanic transform faults: Implications for the spatial distribution of seismicity', *Geochemistry, Geophysics, Geosystems*. John Wiley & Sons, Ltd, 11(7), p. n/a-n/a. doi: 10.1029/2010GC003034.

Le Roux, V. *et al.* (2007) 'The Lherz spinel lherzolite: Refertilized rather than pristine mantle', *Earth and Planetary Science Letters*. doi: 10.1016/j.epsl.2007.05.026.

Sack, R. O. and Ghiorso, M. S. (1989) 'Importance of considerations of mixing properties in establishing an internally consistent thermodynamic database: thermochemistry of minerals in the system Mg2SiO4-Fe2SiO4-SiO2', *Contributions to Mineralogy and Petrology*. doi: 10.1007/BF01160190.

de Saint Blanquat, M. *et al.* (2016) 'Cretaceous mantle exhumation in the central Pyrenees: New constraints from the peridotites in eastern Ariège (North Pyrenean zone, France)', *Comptes Rendus Geoscience*, 348(3–4), pp. 268–278. doi: 10.1016/j.crte.2015.12.003.

Sandu, C., Lenardic, A. and McGovern, P. (2011) 'The effects of deep water cycling on

planetary thermal evolution', *Journal of Geophysical Research*. John Wiley & Sons, Ltd, 116(B12), p. B12404. doi: 10.1029/2011JB008405.

Skogby, H. (2006) 'Water in Natural Mantle Minerals I: Pyroxenes', *Reviews in Mineralogy and Geochemistry*, 62(1), pp. 155–167. doi: 10.2138/rmg.2006.62.7.

Smith, D. (1999) 'Temperatures and pressures of mineral equilibration in peridotite xenoliths: Review, discussion, and implications', in Fei, Y., Bertka, C., and Mysen, B. (eds) *Mantle Petrology: Field Observations and High-Pressure Experimentation*. Washinton D.C.: The Geochemical Society, pp. 171–188.

Spengler, D. *et al.* (2009) 'Long-lived, cold burial of Baltica to 200 km depth', *Earth and Planetary Science Letters*. Elsevier, 281(1–2), pp. 27–35. doi: 10.1016/J.EPSL.2009.02.001.

Szabó, C. *et al.* (2004) 'Composition and evolution of lithosphere beneath the Carpathian–Pannonian Region: a review', *Tectonophysics*. Elsevier, 393(1–4), pp. 119–137. doi: 10.1016/J.TECTO.2004.07.031.

Tatsumi, Y. (1986) 'Formation of the volcanic front in subduction zones', *Geophysical Research Letters*, 13(8), pp. 717–720. doi: 10.1029/GL013i008p00717.

Tatsumi, Y. (1989) 'Migration of fluid phases and genesis of basalt magmas in subduction zones', *Journal of Geophysical Research*, 94(B4), p. 4697. doi: 10.1029/JB094iB04p04697.

Taylor, W. R. (1998) 'An experimental test of some geothermometer and geobarometer formulations for upper mantle peridotites with application to the thermobarometry of fertile lherzolite and garnet websterite', *N Jb Miner Abh*, 172(2–3), pp. 381–408. doi: 10.1127/njma/172/1998/381.

Taylor, W. R. and Green, D. H. (1988) 'Measurement of reduced peridotite-C-O-H solidus and implications for redox melting of the mantle', *Nature*, 332(6162), pp. 349–352. doi:

10.1038/332349a0.

Titus, S. J. *et al.* (2011) ‘Fabric development in the mantle section of a paleotransform fault and its effect on ophiolite obduction, New Caledonia’, *Lithosphere*. doi: 10.1130/L122.1.

Uenver-Thiele, L. *et al.* (2017) ‘Metasomatic processes revealed by trace element and redox signatures of the lithospheric mantle beneath the Massif Central, France’, *Journal of Petrology*, 58(3), pp. 395–422. doi: 10.1093/petrology/egx020.

Vissers, R. L. M. *et al.* (1997) ‘Mylonitic deformation in upper mantle peridotites of the North Pyrenean Zone (France): implications for strength and strain localization in the lithosphere’, *Tectonophysics*. Elsevier, 279(1–4), pp. 303–325. doi: 10.1016/S0040-1951(97)00128-5.

Wallin, E. T. and Metcalf, R. V. (1998) ‘Supra-Subduction Zone Ophiolite Formed in an Extensional Forearc: Trinity Terrane, Klamath Mountains, California’, *The Journal of Geology*, 106(5), pp. 591–608. doi: 10.1086/516044.

Wilshire, H. G. and Trask, N. J. (1971) ‘Structural and texture relationships of amphibole and phlogopite in peridotite inclusions, Dish Hill, California’, *The American Mineralogist*, 56, pp. 240–255.

Wood, B. J. (1990) ‘An experimental test of the spinel peridotite oxygen barometer’, *Journal of Geophysical Research*. Wiley-Blackwell, 95(B10), p. 15845. doi: 10.1029/JB095iB10p15845.

Wood, B. J. (1995) ‘The Effect of H2o on the 410-Kilometer Seismic Discontinuity’, *Science*, 268(5207), pp. 74–76. doi: DOI 10.1126/science.268.5207.74.

Wood, B. J. and Virgo, D. (1989) ‘Upper mantle oxidation state: Ferric iron contents of lherzolite spinels by 57Fe Mossbauer spectroscopy and resultant oxygen fugacities’, *Geochimica Cosmochimica Acta*, 53, pp. 1277–1291.

Woodland, A. B. and Koch, M. (2003) ‘Variation in oxygen fugacity with depth in the upper

mantle beneath the Kaapvaal craton, Southern Africa', *Earth and Planetary Science Letters*. doi: 10.1016/S0012-821X(03)00379-0.

Woodland, A. B., Kornprobst, J. and Wood, B. J. (1992) 'Oxygen Thermobarometry of Orogenic Lherzolite Massifs', *Journal of Petrology*. Oxford University Press, 33(1), pp. 203–230. doi: 10.1093/petrology/33.1.203.

Wu, C. M. and Zhao, G. C. (2007) 'A recalibration of the garnet-olivine geothermometer and a new geobarometer for garnet peridotites and garnet-olivine-plagioclase-bearing granulites', *Journal of Metamorphic Geology*, 25(5), pp. 497–505. doi: 10.1111/j.1525-1314.2007.00706.x.

Wyllie, P. J. (1971) 'Role of Water in Magma Generation and Initiation of Diapiric Uprise in Mantle', *Journal of Geophysical Research*, 76(5), pp. 1328-. doi: DOI 10.1029/JB076i005p01328.

Wyllie, P. J. (1977) 'Effects of H2O and CO2 on magma generation in the crust and mantle', *Journal of the Geological Society*, 134(2), pp. 215–234. doi: 10.1144/gsjgs.134.2.0215.

Xu, Y., Lin, C. and Shi, L. (1999) 'The geotherm of the lithosphere beneath Qilin, SE China: A re-appraisal and implications for P-T estimation of Fe-rich pyroxenites', *Lithos*, 47(3–4), pp. 181–193. doi: 10.1016/S0024-4937(99)00014-6.

Zhao, Y. H., Ginsberg, S. B. and Kohlstedt, D. L. (2004) 'Solubility of hydrogen in olivine: Dependence on temperature and iron content', *Contributions to Mineralogy and Petrology*, 147(2), pp. 155–161. doi: 10.1007/s00410-003-0524-4.

APPENDIX

All mineral composition data can be found in the electronic supplementary materials accompanying this thesis.